



Submitted for

National Science, Technology and Innovation Plan

**New Methods to Improve Seismic Ground Motion
Predictions and Seismic Hazard in Saudi Arabia**

(REVISED FINAL)

Project No. : 09 – INF 945-02

Prof. Abdullah M. Al-Amri (PI)

Dr. Mohammed S. Fnais (CO - I)

Dr. Michael Pasyanos (CO – I)

January 4, 2013

Abstract

We applied new methods to characterize and model earthquake ground motions in Saudi Arabia. This research will result in greatly improved characterization of the laterally varying attenuation properties of Arabian Peninsula across a broad frequency range and a predictive capability for ground motions for scenario future earthquakes. We performed a high-resolution tomographic inversion of high-frequency regional P-wave and S-wave amplitudes to provide a physics-based attenuation relation for the entire SA. We also modeled long-period ground motions along the Arabian Gulf coast from large earthquakes in the Zagros Mountains to understand the high amplitude and long-duration shaking from these events. Analysis involved: 1) collection of three-component seismograms from regional events in and around Saudi Arabia; 2) modeling of the long-period waveforms for source parameters (focal mechanism, depth, seismic moment); 3) measurement of the regional phase amplitudes; 4) modeling of the amplitude spectra for average (one-dimensional) attenuation behavior; 5) tomographic inversion of amplitude residuals for two-dimensional maps of velocity, along with attenuation (Q_p and Q_s) of the crust and upper mantle as a function of frequency.

Generally, exceptionally long-duration seismic waves, as compared with standard models, are shown to occur with periods of 1-10 seconds. This may be due to waveguide effects in the sedimentary basin. In Task 4, “*Modeling of Long-Period Ground Motions in the Gulf,*” we performed 3D wave propagation simulations using finite difference calculations and four basin models, including a preliminary version of model LITHO1.0, with different shallow sedimentary layer structures. The modeling results confirm our hypothesis that long period waves with extremely long duration and relatively large amplitudes are controlled by the geometry of the top basin sedimentary layers and source depth. Combined effects of basin edge geometry with sharp velocity contrast and shallow sources ($< 10\text{km}$) on the east part of the Arabian Gulf can cause large long period ground motion on the west part of the Gulf basin.

Acknowledgments

The authors would like to express their thanks and gratitude to the National Plan for Science, technology and innovation at KACST for funding this project (**Grant no. 09 – INF945-02**). We extend our sincerest thanks to Dr. Arben Pitarka, Robert Mellors and Arthur Rodgers for their contributions and to Mr. Mostafa Hemida, Musaed Al-Harbi and Omar Loni for their supervising construction of seismic stations and data collection.

Table of Contents

Abstract

Acknowledgments

1. Introduction.....	8
2. Objectives.....	9
3. Seismotectonic Setting.....	12
4. Methods & Materials.....	17
4.1 Regional-Phase Attenuation.....	17
4.2 Amplitude Tomography.....	17
4.3 Application to Earthquake Hazard.....	18
4.4 Source Parameters.....	23
4.5 Long-period Ground Motions in the Gulf.....	24
5. Results & Data Analysis.....	32
5.1 Data Collection.....	32
5.2 Determine Source Parameters.....	32
5.3 Measure Regional Phase Amplitudes.....	36
5.4 Tomographic Imaging for 2D Velocity and Attenuation Maps.....	39

6. Discussion & Interpretation.....	42
6.1 Interpreted Seismicity of the Gulf Region.....	42
6.2 Analysis of Long-Period Ground Motions in the Gulf.....	45
6.3 Recorded Spectral Response Characteristics.....	50
6.4 Modeling of Long-Period Ground Motions in the Gulf.....	56
6.5 3D Ground Motion Simulation.....	57
6.6 Ground Motion Simulation Using LITHO1.0.....	64
Summary & Conclusions.....	68
References.....	71
Publications / Presentations.....	75

List of Figures

Fig. No.	Subject	Page No.
3.1	Seismotectonic map of the Arabian Peninsula	16
4.1	Paths for regional phases Pn ,Pg , Sn , and Lg in the Middle East	20
4.2	Maps of attenuation quality factor Q for shear waves in the crust	21
4.3	Broadband stations from the KACST and SGS networks	22
4.4	Hypothetical spectral accelerations from a Mw 6.5 event	26
4.5	Example of waveform fitting for an event in Turkey	27
4.6	Map of events for which we have modeled source parameters in the Turkish-Iranian Plateau	29
4.7	Map of the November 27, 2005 Qeshm Island earthquake, focal mechanism and paths to station HASS	30
4.8	Observed transverse component ground motion from the Nov. 22, 2005 Qeshm Island event at station HASS	31
5.1	SNSN stations and regional earthquakes for which we have already made phase amplitude measurements	33
5.2	The Ar-Rayn seismic array. Each element in the array is a three-component broadband station.	34
5.3	left panel shows misfit, moment tensor solution, and moment magnitude as a function of depth.	37
5.4	Map of regional moment tensor solutions determined using the Cut-and-Paste method.	38
5.5	Surface Wave Dispersion: (left) path map including regional stations (red) and earthquakes (yellow) used for a tomographic inversion (right) of the Rayleigh wave dispersion data at 20 seconds period	40
5.6	Surface Wave Attenuation: Path map (left) and initial result (right) for a surface wave inversion of the 25 second period Rayleigh wave	41
6.1	Seismicity of the Arabian Platform and adjacent regions (1980 - 2010).	44
6.2	Map of study area showing earthquakes and seismic stations.	46
6.3	Sediment thickness of the Arabian Gulf and surrounding region.	47
6.4	Seismograms for 3 June, 2006 earthquake recorded at stations in eastern Saudi Arabia filtered (a) 0.02-0.05 Hz (50-20 seconds) and (b) 0.1-1.0 Hz (10-1 seconds).	49
6.5	Spectral acceleration ratios of recorded and predicted ground motion for the geometric mean horizontal component at periods 1s,	53

	5s, and 10s, and 5% damping.	
6.6	Mean spectral acceleration ratios of recorded and predicted ground motion at periods of 1s, 5s, and 5% damping.	54
6.7	Acceleration response spectra for ground motion from M 5.3 2006/06/03 earthquake (top panels), M5.7 2010/07/20 (middle panels), M 5.9 2010/09/27 (bottom panels), recorded at different stations in the Gulf region.	55
6.8	Vertical cross sections of three velocity models used in the simulation of basin generated waves.	58
6.9	Synthetic velocity seismograms computed for a double couple point source with a thrust mechanism using Model 1 (left panels) Model 2 (central panels), and Model 3 (right panels). The seismograms are band-pass filtered at 0.01-0.4 Hz.	60
6.10	Synthetic velocity seismograms computed for a double couple point source with a thrust mechanism using Model 1 (left panels) and Model 2 (central panels), and Model 3 (right panels). The seismograms are band-pass filtered at 0.2-0.4 Hz.	61
6.11	Comparison acceleration response spectra of synthetic seismograms shown in Figure 6.9 for Model 1(red traces), Model 2(blue traces), and Model 3(green traces).	63
6.12	Vertical cross section of the tomographic model used in the simulation of basin-generated waves.	65
6.13	Synthetic velocity seismograms computed for a double couple point source with a trust mechanism using tomographic model.	66
6.14	Comparison of acceleration response spectra of synthetic seismograms computed with the tomographic model and three other basin models.	67

1. Introduction

Saudi Arabia is an area which is characterized very poorly seismically and for which little existing data is available. While for the most part aseismic, the area is ringed with regional seismic sources in the tectonically active areas of Iran and Turkey to the northeast, the Red Sea Rift bordering the Shield to the southwest, and the Dead Sea Transform fault zone to the north. Throughout recorded history many damaging earthquakes have occurred along the Arabian Plate boundaries. These events have damaged buildings, and resulted in injuries and fatalities. There is obviously potential for damaging earthquakes in the future. As the population increases and new areas are developed, the seismic risk to human life and infrastructure increases.

While the KSA is relatively aseismic, large devastating earthquakes have occurred. Specifically the Gulf of Aqaba has had many large damaging earthquakes, including the November 22, 1995 M_w 7.2 event and most recently the June 22, 2005 M_w 5.1 Tabuk (Al Damegh et al., 2008) and May 19, 2009 M_w 6.1 Umm Laj events. Furthermore, large earthquakes in the Zagros Mountains can cause shaking in buildings along the Gulf coast. On June 2, 1993, an earthquake of magnitude 4.7 occurred in Kuwait near the Minagish oil field. In spite of its modest magnitude, the earthquake was widely felt and caused panic in the city of Kuwait. More recent events in the Minagish area include a magnitude 3.9 earthquake on September 18, 1997 and a magnitude 4.2 event on December 30, 1997. On January 2002 a moderately large earthquake shook the Musadam Peninsula on the border region of Oman and the United Arab Emirates. Another major source is the Makran subduction zone, located at the southern end of the plate boundary, where the Arabian plate around the Gulf of Oman subducts underneath the Eurasian plate. Such subduction zones can create very large earthquakes. The great Makran earthquake of November 1945 had a magnitude of 8.1. While seismologists rely on average attenuation relationships for

different regions, these often fail to predict actual shaking behavior. Attenuation relationships typically apply to high-frequency shaking, above 1 Hz. Shaking at lower-frequencies is more complex because three-dimensional elastic structure can cause dispersion, focusing and amplification in a deterministic fashion. Fortunately, the state-of-the-art national seismic network operated by the Saudi Geologic Survey (SGS) provides excellent data for determining path-dependent attenuation properties of Arabian Peninsula.

The Arabian Gulf is adjacent to one of the most seismically active fold-and-thrust belts on Earth, the Zagros Mountains. Broadband seismic records of earthquakes in the Zagros Mountains recorded on the Arabian side of the Gulf display long duration surface waves. While shorter periods (< 1 s) are attenuated from crossing the deep sediments (> 10 km) of the Gulf basin, the long period energy is relatively unaffected. Consequently large earthquakes in the Zagros could result in possibly damaging ground motions at long-periods (1-10 s). Such ground motions are of concern for large engineered structures, such as tall buildings and long bridges with resonant periods in the same frequency band (period of 1-10 s).

2. Objectives

Observations from past earthquakes have shown that, long-period, long-duration shaking created by distant earthquakes cause tall buildings undergo a large number of stress reversals, resulting in strength deteriorations in concrete elements and fatigue failures in steel connections. The impact of an earthquake is not limited to direct losses, such as the loss of life, loss of structures, and business interruptions. Earthquakes also cause indirect losses by producing supply shortages and demand reductions in various economic sectors.

This proposal seeks to analyze recently recorded broadband seismic data to determine path-specific attenuation properties of earthquakes and improve seismic hazard assessment. Because of the structure of the Earth is complex the attenuation or decrease in shaking amplitude with distance from an earthquake is strongly dependent on the crustal structure between the source and point of interest. Furthermore, the detailed structure of crust along any path is poorly known and cannot be easily determined for all possible paths between earthquake sources and points where we wish to estimate ground shaking. This project will result in improved attenuation models and microzonation of the Arabian Peninsula.

The goals of this are threefold:

- ❖ Improve monitoring capability in the region,
- ❖ Provide a better understanding of the geophysics and tectonics of the region,
- ❖ Ground motion prediction and hazard analysis.

Analysis of high-frequency ground motions will result in a model of path and frequency dependent attenuation across the entire Arabian Peninsula with high-resolution in populated regions well covered by SGS stations in the Arabian Shield. Results can be used to create attenuation relationships for source, site and path-specific conditions. Furthermore, we will characterize and model long-period ground motions from earthquakes in the Zagros Mountains and investigate the hazard they pose to large engineered structures (e.g. tall buildings, long bridges and pipelines). This will allow for improved accuracy of earthquake ground motion amplitudes and more realistic seismic hazard for the Kingdom.

PROJECT WORK PLAN

PHASES & TASKS	INVOLVEMENT DURATION	1	2	3	4	5	6	7	8	9	10	11	12	13	14	15	16	17	18	19	20	21	22	23	24
		PHASE I																							
Task 1.1:	Data Collection	█	█	█																					
Task 1.2:	Source Parameters				█	█	█																		
PHASE 2																									
Task 2.1	Regional Phase amplitudes							█	█	█															
Task 2.2	Tomographic Imaging for 2D										█	█	█	█	█	█									
PHASE 3																									
	Analysis of long-period ground motions																								
PHASE 4																									
	Modeling of long-period ground motions																				█	█	█	█	█

3. Seismotectonic Setting

The Arabian Peninsula forms a single tectonic plate, the Arabian Plate. It is surrounded on all sides by active plate boundaries as evidenced by earthquake locations. **Figure 3.1** shows a map of the Arabian Peninsula along with major tectonic features and earthquake locations. Active tectonics of the region are dominated by the collision of the Arabian Plate with the Eurasian Plate along the Zagros and Bitlis Thrust systems, rifting and seafloor spreading in the Red Sea and Gulf of Aden. Strike-slip faulting occurs along the Gulf of Aqabah and Dead Sea Transform fault systems. The great number of earthquakes in the Gulf of Aqabah pose a significant seismic hazard to Saudi Arabia. Large earthquakes in the Zagros Mountains of southern Iran may lead to long-period ground motion in eastern Saudi Arabia.

The accretionary evolution of the Arabian plate is thought to have originated and formed by amalgamation of five Precambrian terranes. These are the Asir, Hijaz, and Midyan terranes from the western part of the Arabian shield, and from the eastern side of the shield are the Afiferrane and the Amar arc of the Ar Rayn micro-plate. The western fusion is along the BirUmq and Yanbu sutures (Loosveld et al 1996). The eastern accretion may have started by about 680-640 million years ago (Ma) when the Afif terrane collided with the western shield along the Nabitah suture. At about 670 Ma, a subduction complex formed west of Amar arc. Along this subduction zone, the Afif terrane and ArRayn microplate collided that lasted from about 640-620 Ma. (Al-Husseini 2000). The north trending Rayn anticlines and conjugate northwest and northeast fractures and faults may have formed at this time.

The Arabian Shield is an ancient land mass with a trapezoidal shape and area of about 770,000 sq. km. Its slightly-arched surface is a pen plain sloping very gently toward the north, northeast, and east. The framework of the shield is composed of Precambrian rocks and metamorphosed

sedimentary and intruded by granites. The fold-fault pattern of the shield, together with some stratigraphic relationships suggests that the shield have undergone two orogenic cycles.

To the first order, the Arabian shield is composed of two layers, each about 20 km thick, with average velocities of about 6.3 km/s and 7 km/s respectively (Mooney et al 1985). The crust thins rapidly to less than 20 km total thickness at the western shield margin, beyond which the sediments of the Red Sea shelf and coastal plain are underlain by oceanic crust.

The platform consists of the Paleozoic and Mesozoic sedimentary rocks that unconformably overlays the shield and dip very gently and uniformly to the E-NE towards the Arabian Gulf (Powers et al., 1966). The accumulated sediments in the Arabian platform represent the southeastern part of the vast Middle east basin that extend eastward into Iran, westward into the eastern Mediterranean and northward into Jordan, Iraq and Syria.

The Arabian shield isolated the Arabian platform from the north African Tethys and played an active paleogeographic role through gentle subsidence of its northern and eastern sectors during the Phanerozoic, allowing almost 5000 m of continental and marine sediments deposited over the platform. This accumulation of sediments represents several cycles from the Cambrian onward, now forms a homocline dipping very gently away from the Arabian shield.

Several structural provinces can be identified within the Arabian platform : 1) An interior homocline in the form of a belt, about 400 km wide, in which the sedimentary rocks dip very gently away from the shield outcrops. 2) An interior platform, up to 400 km wide, within which the sedimentary rocks continue to dip regionally away from the shield at low angles. 3) Intra-shelf depressions, found mainly around the interior homocline and interior platform .

The Saudi Arabian Broadband Deployment (Vernon and Berger, 1997; Al-Amri et al., 1999) provided the first broadband recordings for the Arabian Shield and Platform. This deployment

consisted of 9 broadband, three-component seismic stations along a similar transect to a seismic refraction study (Mooney et al., 1985; Gettings et al., 1986; Badri, 1991). Data from this deployment resulted in several reports of crustal and upper mantle structure (Sandvol et al., 1998; Mellors et al., 1999; Rodgers et al., 1999; Benoit et al., 2003; Mokhtar et al., 2001). The crustal model of the western Arabian Platform shows a slightly higher P-velocity for the upper crust in the Arabian Shield than in the Platform. Also the crust of the Platform appears to be 3-5 km thicker than in the Shield. The Moho Discontinuity beneath the western Arabian Platform occurs at a depth of 40-45 km, and the velocity of the upper mantle is about 8.2 km/sec (Al-Amri 1998; 1999; Rodgers et al., 1999; Tkalcić et al., 2006).

Generally, the crustal thickness in the Arabian Shield varies from about 15 km in the Red Sea, to 20 km along the Red Sea coast to about 35-40 km in the in central Arabian Shield (Sandvol et al., 1998; Al-Damegh et al., 2005; Tkalcić et al., 2006). Reports of large-scale seismic tomography (e.g. Debayle et al., 2001) suggest that a low-velocity anomaly in the upper mantle extends laterally beneath the Arabian Shield from the Red Sea in the west to the Shield-Platform boundary in the east. Additionally, Debayle et al. (2001) observed a narrow region of low-velocity beneath the Red Sea and the western edge of the Arabian Shield, extending to 650 km depth. Recent tomographic imaging by Park et al. (2007) using SANDSN data found low velocities extending to 400 km in the upper mantle beneath the southern Red Sea and Arabian Shield, but more normal velocities beneath the northern Red Sea, suggesting different geodynamic connections between rifting of the Red Sea and mantle upwelling in the southern and northern Red Sea.

High-frequency regional S-wave phases are quite different for paths sampling the Arabian Shield than those sampling the Arabian Platform (Mellors et al., 1999; Al-Damegh et al., 2004). In

particular the mantle Sn phase is nearly absent for paths crossing parts of the Arabian Shield, while the crustal Lg phase has abnormally large amplitude. This may result from an elastic propagation effect or extremely high mantle attenuation and low crustal attenuation occurring simultaneously, or a combination of both. High-frequency Lg does not propagate as efficiently across the Arabian Platform compared to the Shield but Sn does propagate efficiently. This suggests that crustal attenuation is low in the higher velocity crust of the Arabian Shield, or sedimentary structure in the Arabian Platform attenuates and disrupts the crustal waveguide for Lg. These observations imply high-frequency ground motions will propagate with lower attenuation in the Arabian Shield compared to the Arabian Platform.

It is known that high-frequency regional phase behavior in the Arabian Plate is quite variable as demonstrated by Al-Damegh et al. (2004). They investigated the attenuation of P_n phase (Q_{P_n}) for 1–2 Hz along the Red Sea, the Dead Sea fault system, within the Arabian Shield and in the Arabian Platform. Consistent with the Sn attenuation, they observed low Q_{P_n} values of 22 and 15 along the western coast of the Arabian Plate and along the Dead Sea fault system, respectively, for a frequency of 1.5 Hz. Higher Q_{P_n} values of the order of 400 were observed within the Arabian Shield and Platform for the same frequency. Their results based on Sn and P_n observations along the western and northern portions of the Arabian Plate imply the presence of a major anomalously hot and thinned lithosphere in these regions that may be caused by the extensive upper mantle anomaly that appears to span most of East Africa and western Arabia.

More recently, Pasyanos et al. (2009) applied a technique to simultaneously invert amplitudes measurements of Pn, Pg, Sn and Lg to produce P-wave and S-wave attenuation models of the crust and upper mantle. The attenuation is modeled as P-wave and S-wave attenuation surfaces for the crust, and similar set for the upper mantle. They used all of the phase amplitudes together

by using the appropriate (source, geometrical-spreading, site, and attenuation) terms for each phase. Because this is a model-based inversion, the velocity structure of the region can be included to more accurately model the predicted ray paths.

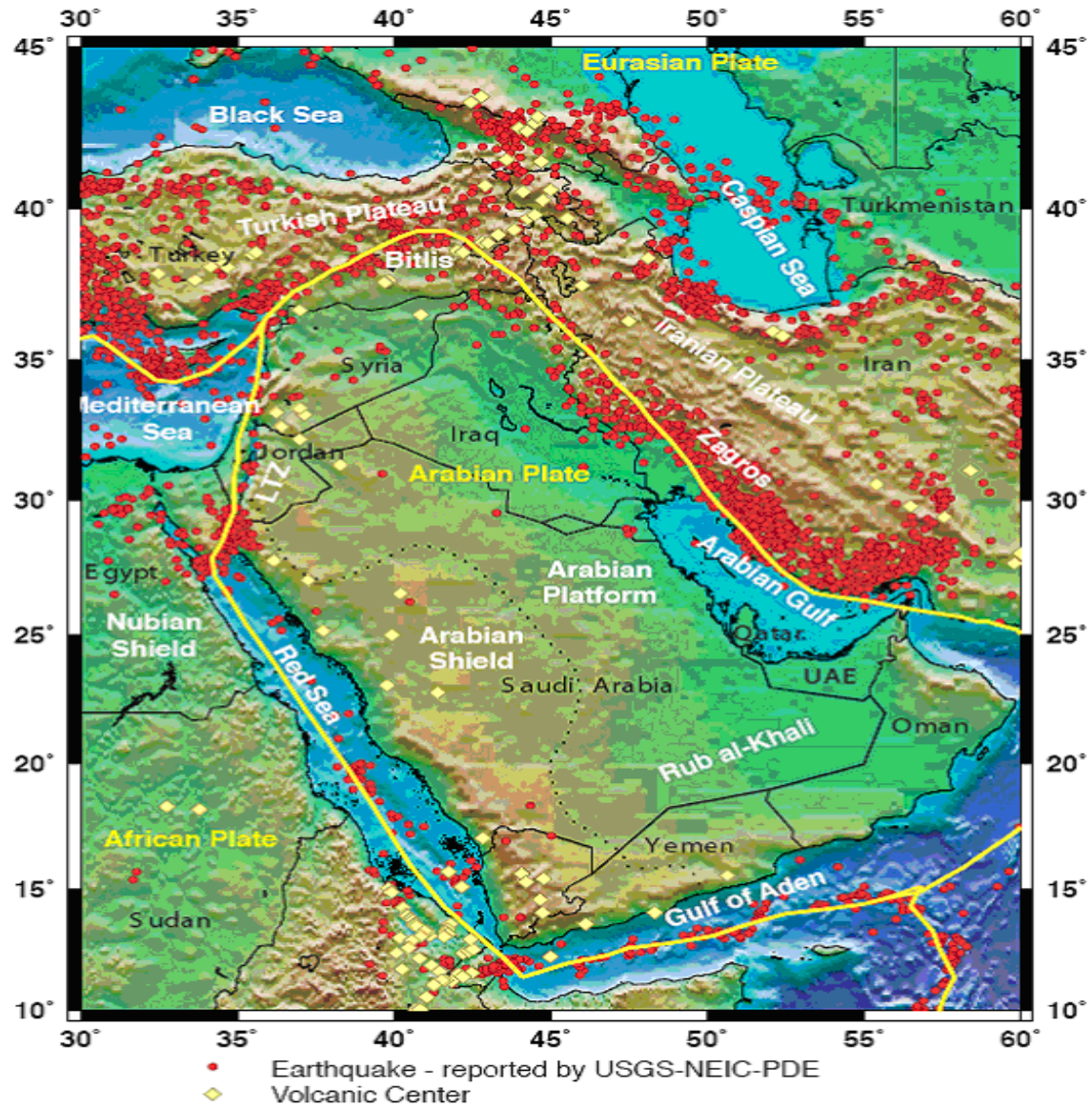


Figure 3.1 Seismotectonic map of the Arabian Peninsula and Arabian plate boundaries.

4. Methods & Materials

4.1 Regional-Phase Attenuation

In a subsequent paper (Pasyanos et al., 2009b) applied the technique to simultaneously invert amplitudes measurements of Pn, Pg, Sn and Lg (**Figure 4.1**) to produce P-wave and S-wave attenuation models of the crust and upper mantle (**Figure 4.2**). The attenuation is modeled as P-wave and S-wave attenuation surfaces for the crust, and a similar set for the upper mantle. We can use all of the phase amplitudes together by using the appropriate (source, geometrical-spreading, site, and attenuation) terms for each phase. For example, the source terms of the P-waves and S-waves are different, and path attenuation is calculated by ray paths appropriate for the particular phase. Inverting all of the phases simultaneously (in this case, amplitudes for about 12,000 paths) allows us to determine consistent attenuation, site, and source terms for all phases, and eliminates non-physical inconsistencies among them. As a result, we can now predict the amplitudes of any of these regional phases for an event of any given location and size. It is known that high-frequency regional phase behavior in the Arabian Plate is quite variable as demonstrated by Al-Damegh et al. (2004). This study will use more quantitative measures of phase attenuation.

4.2 Amplitude Tomography

In the tomography that we have developed (Pasyanos et al., 2009a, 2009b), the amplitudes are modeled as the product of a source term S , a geometrical spreading term G , an attenuation term B , and a site term P . In the frequency domain, this is usually represented by the expression:

$$A_{ij} = S_i G_{ij} B_{ij} P_j. \quad (1)$$

The inversion is performed by assuming a geometrical spreading, setting initial values for the other terms, and solving for source and site terms along with lateral attenuation. For earthquakes,

we adopt an MDAC source model (Walter and Taylor, 2001) which is easily relatable to seismic moment M_0 . For P- and S-waves the earthquake source terms are, respectively:

$$\begin{aligned} S^P &= F^P M_0 / (1 + (\omega / \omega_c^P)^2), \\ S^S &= F^S M_0 / (1 + (\omega / \omega_c^S)^2), \end{aligned} \quad (2)$$

where ω_c is the corner frequency, and F for P-waves and S-waves is specified as:

$$\begin{aligned} F^P &= R_{\theta\phi}^P / 4\pi \sqrt{\rho_s \rho_r \alpha_s^5 \alpha_r}, \\ F^S &= R_{\theta\phi}^S / 4\pi \sqrt{\rho_s \rho_r \beta_s^5 \beta_r} \end{aligned} \quad (3)$$

By making reasonable assumptions about these parameters and the relative corner frequencies of the P-waves and S-waves ($\omega_c^P = \omega_c^S$), we find $F^S = 6.89 F^P$ and $S^S = 6.89 S^P$ (Pasyanos et al., 2009b). This allows us to use both P-wave and S-wave amplitude data and solve for one source term. Specifying a $\omega_c^P \neq \omega_c^S$ relation simply makes the source term ratio a function of the corner-frequency or moment of the event.

4.3 Application to Earthquake Hazard

While maps of the seismic attenuation of the crust and upper mantle of Saudi Arabia are very good at low frequencies (0.5-1, 1-2 Hz), maps at high frequencies are significantly worse due to the higher amplitude falloff at these frequencies and generally low seismicity rate of the Kingdom. This is unfortunate, as estimating the attenuation at high frequencies is essential for predicting the largest ground motions of damaging earthquakes. Making amplitude at high-frequencies requires either larger events, closer observing distances, or both. By using the seismic networks of both KACST and SGS (**Figure 4.3**), we will be able to make amplitude measurements throughout Saudi Arabia, particularly at high-frequencies, which can then feed

into the attenuation tomography. Along with information on the velocity structure, this can have a large effect on predicted ground motions.

As shown in **Figure 4.4**, there are significant differences in the shear-wave attenuation of the crust (Crustal Q_s panel) between low Q (high attenuation) of the Red Sea and Zagros Mts. and the high Q (low attenuation) of the Arabian Shield and Arabian Platform. **Figure 4.4** shows hypothetical spectral accelerations from a Mw 6.5 event at 50 km distance from an observed Lg phase. This figure is calculated by determining the predicted displacement amplitudes in each frequency band and converting the displacements to acceleration. Lines correspond to expected accelerations for different values of crustal Q . Similar figures could be prepared for other regional phases. Attenuation will affect both the overall level of shaking as well as the frequency content. In **Figure 4.4**, we see differences close to a factor of 3 near 2 Hz and even larger factors at higher frequencies. Besides high-resolution attenuation maps, another important factor in predicting ground motions will be local site effects. This is also captured in the inversion through the site term P .

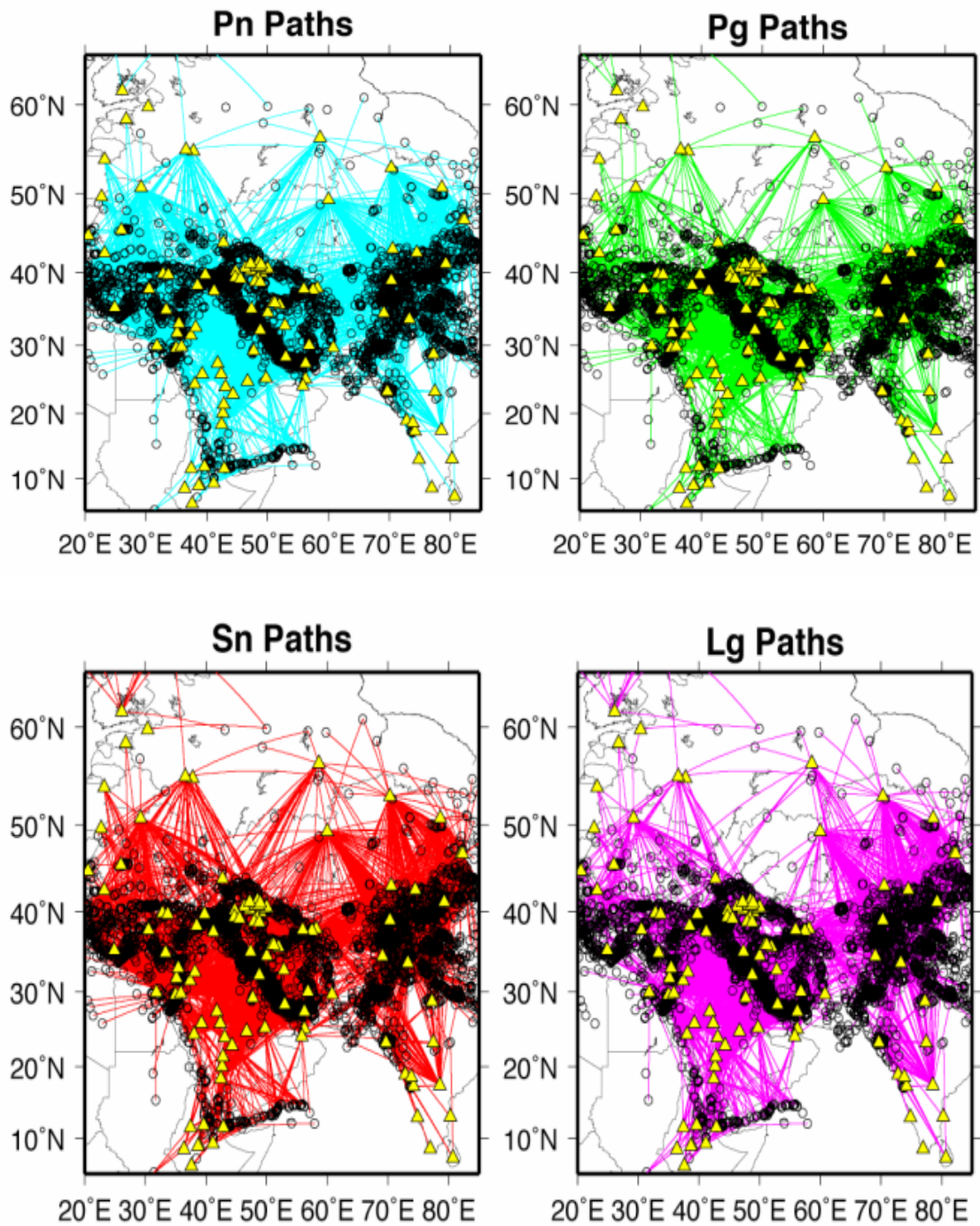


Figure 4.1. Paths for regional phases Pn (cyan), Pg (green), Sn (red), and Lg (magenta) in the Middle East region in the 1-2 Hz passband along with stations (yellow triangles) and events (black circles). Figure from Pasyanos et al. (2009b).

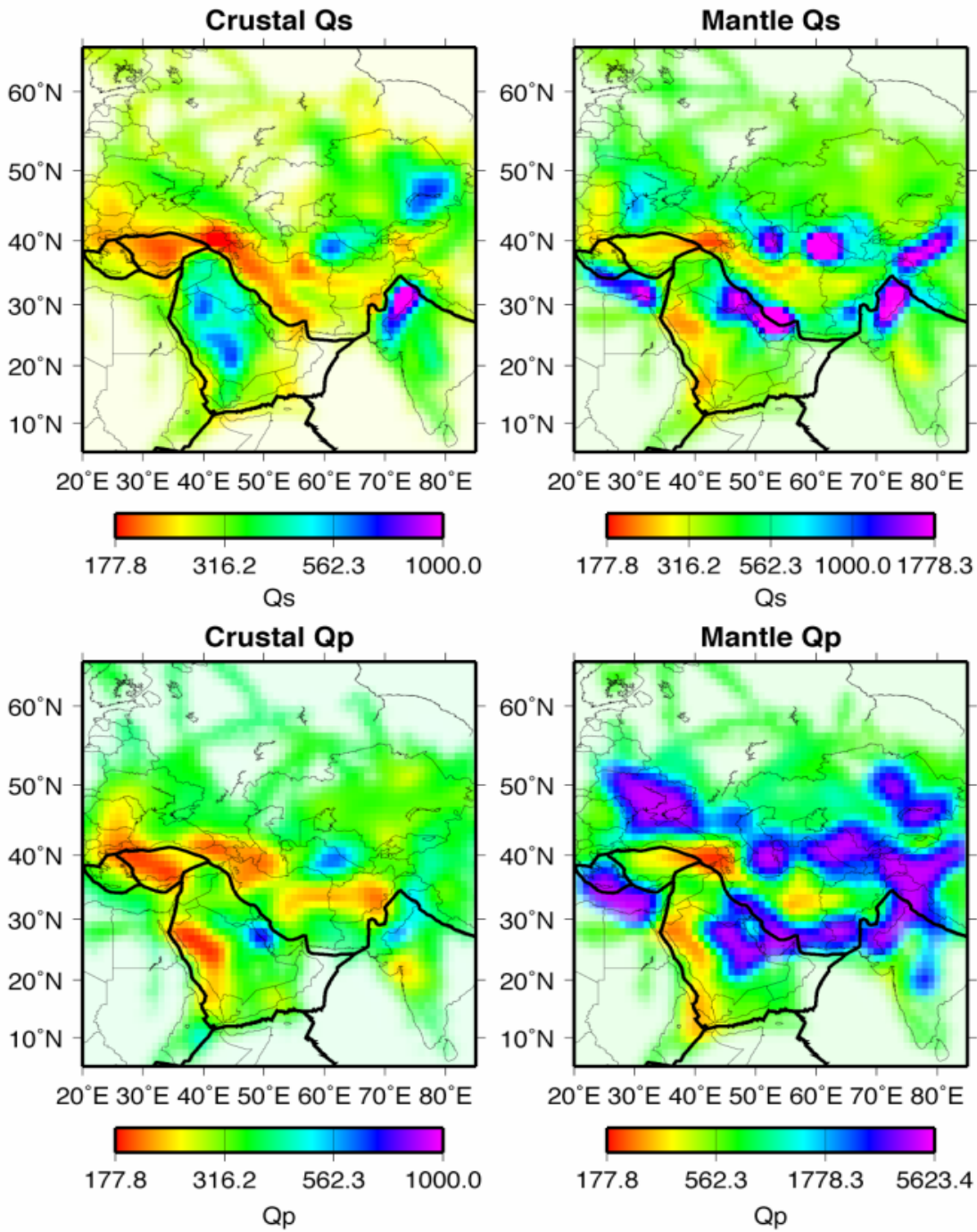


Figure 4.2. Maps of attenuation quality factor Q for shear waves in the crust (crustal Q_s), shear waves in the mantle (mantle Q_s), compressional waves in the crust (crustal Q_p), and compressional waves in the mantle (mantle Q_p) in the 1-2 Hz passband. Figure from Pasyanos et al. (2009b).

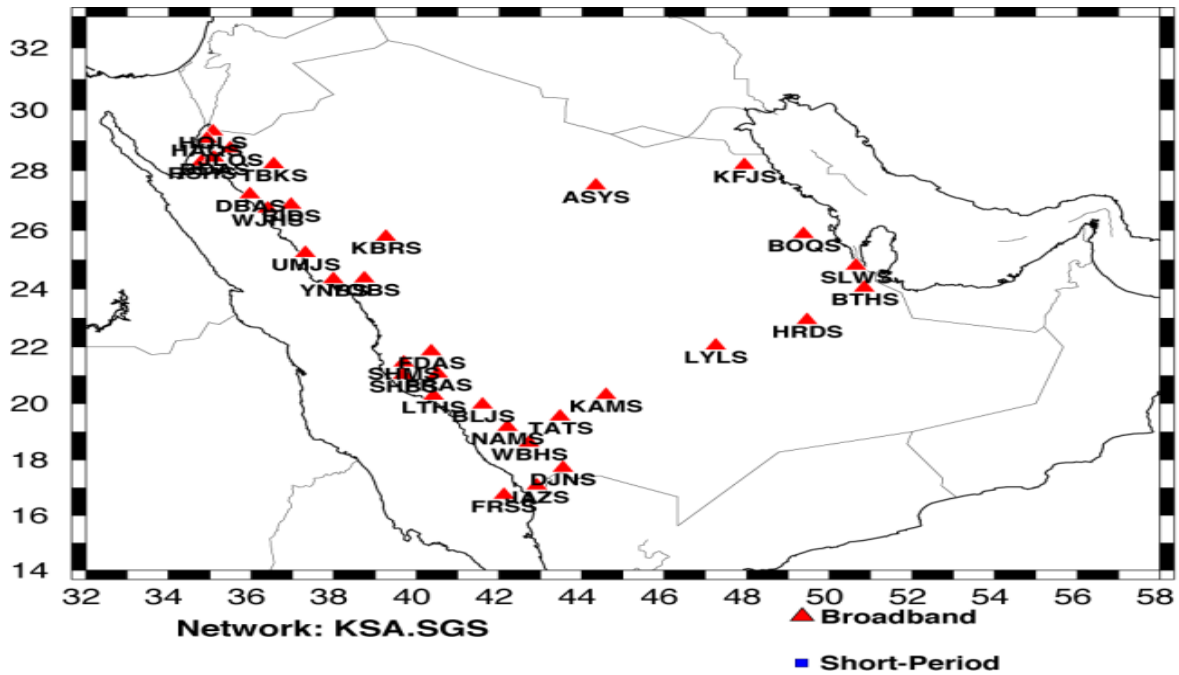
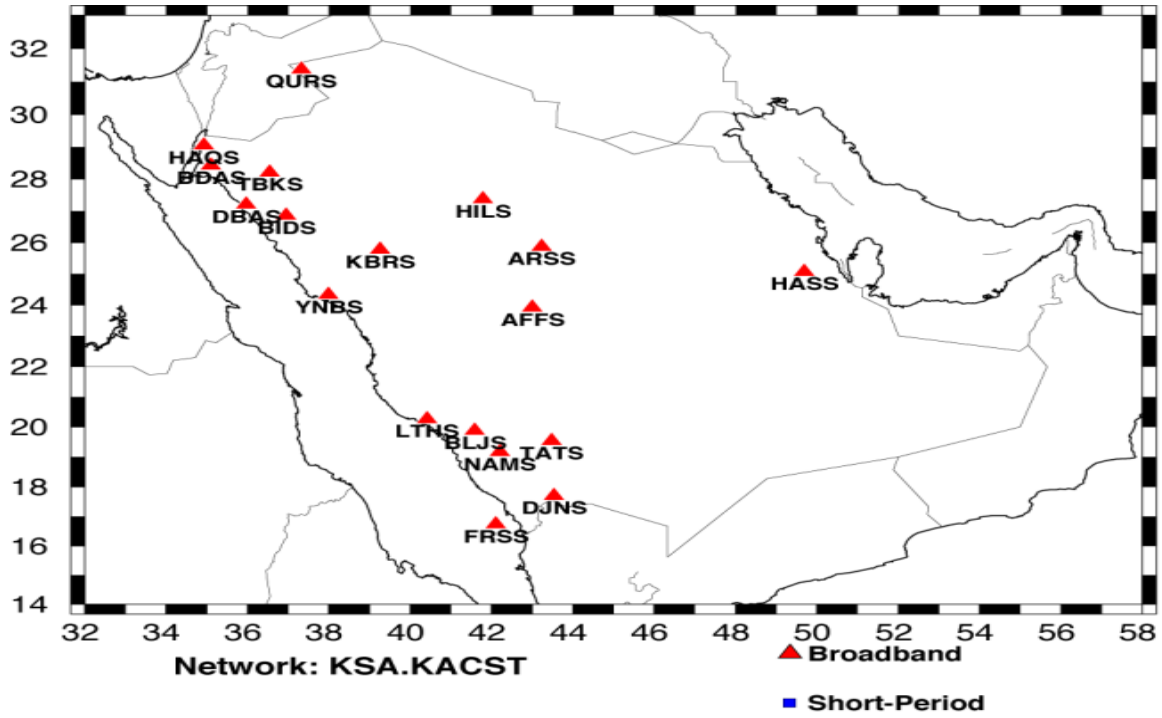


Figure 4.3. Broadband stations from the KACST (left) and SGS (right) networks which would be used to improve amplitude path coverage of the Kingdom.

4.4 Source Parameters

The physics-based modeling of regional phase amplitudes to estimate attenuation as described above requires us to use a model of the source amplitude spectrum. The low-frequency level of the source spectrum depends on the seismic moment. We propose to model the complete local and regional distance three-component waveforms to estimate the seismic moment, depth and focal mechanism. We will use proven methods based on grid search with Green's functions for a one-dimensional (plane-layered) seismic wave speed and density model. We have used methods based on grid-search for the best double-couple (e.g. Walter, 1993) or full moment tensor inversion (e.g. Dreger and Helmberger, 1993; Ritsema and Lay, 1995; Al Damegh et al., 2009). Recently, we have used a method, called "Cut-and-Paste" (CAP) for modeling regional waveforms for the best double-couple mechanisms, moment and depth (Zhao and Helmberger, 1994; Zhu and Helmberger, 1996). This method breaks the regional waveforms into five segments for the Pn1, Rayleigh and Love waves and allows for shifting of the segments to account for errors in the assumed 1D seismic structure. **Figure 4.5** shows the application of the CAP method for an earthquake in western Turkey. The waveform segments are plotted separately with the observed (blue) and synthetic (red) shifted to improve the alignment. The method finds the best mechanism and seismic moment (moment magnitude) at a number of depths. The best solution is taken as the minimum misfit for all depths.

The CAP method requires that we use a good average 1D seismic waves peed and density model. We will work with a few well characterized events that sample the region to test our models from previous work (Rodgers et al., 1998; Al-Amri et al., 2008). We have applied the CAP method for a set of events in the Turkish-Iranian Plateau. **Figure 4.6** shows the focal mechanisms in map view for about 100 events. Some of these events in the southern Zagros may

be used for this study if we can obtain the associated broadband recordings from Saudi stations. We expect the event set would include events from the seismic activity that surrounds the Kingdom: the Dead Sea Fault, Gulf of Aqaba, Red Sea, Gulf of Aden, Owen Fracture Zone, Zagros and Bitlis Thrust zones. Also important would be the seismicity within the Kingdom such as the June 22, 2005 M_w 5.1 Tabuk (Al Damegh et al., 2008), May 19, 2009 M_w 6.1 Umm Laj (Harrat Lunyar) and events in the Al-Hasa region events.

4.5 Long-period Ground Motions in the Gulf

In a recent study we demonstrated that the sedimentary geology of the Arabian Gulf causes higher amplitude and longer duration ground shaking than would be expected in more normal continental crustal structure. The most seismically active region near Saudi Arabia is the Zagros Thrust Belt, where convergence between the Arabian and Eurasian Plates is expressed in frequent earthquakes. Large ($M > 6.0$) events occur on average at least once a year or more frequently in this region; however, these events are 200 km or greater from the Arabian coast. Ground motion hazard for such large distances is unusual. Nonetheless, ground motions caused by distant events in the Zagros have resulted in felt motions in tall buildings in cities along the Arabian coast. An example of this is the November 22, 2005 M 5.7 Qeshm Island. This event caused motions in tall buildings in Dubai, United Arab Emirates, and other cities along the Gulf coast.

Data recorded by the SANDSN allows us to document and understand the nature of these ground motions. **Figure 4.7a** shows the location of the Qeshm Island event, focal mechanism, and paths to stations HASS (Al-Hasa, Kingdom of Saudi Arabia) and ZHSF (Iran). The transverse component seismograms from this event recorded at stations HASS and ZHSF, and filtered 0.1–0.3 Hz are shown in **Figure 4.7**. The paths to these stations should have relatively equal Love-

wave radiation due to the paths leaving symmetric sides of the focal mechanism. However, note that the ground motions at HASS are of larger amplitude and longer duration than those at ZHSF. The path to HASS passes through the thick sedimentary cover in the Arabian Gulf. Similar observations have been seen for other events recorded at HASS. Long-period ground motions are more likely to impact large structures because the resonant period of large structures is longer than small structures.

To understand the nature of the long-duration, high-amplitude ground motions, we modeled these seismograms with a 3D model using the spectral element method (SEM) code developed by Komatitsch and Tromp (2002ab). We used the 3D model reported by Shapiro and Ritzwoller (2002), which is based on surface wave dispersion and the sedimentary basin thickness reported by Laske and Masters (1997). **Figure 4.8** shows the observed and synthetic seismograms resulting from the SEM calculations for the 3D model and the 1D (or depth-dependent) iasp91 model (Kennett and Engdahl 1991). These calculations require parallel computing to perform the calculations to sufficient resolution. Calculations to frequencies of 0.2 Hz can be performed on modern LINUX cluster of 64 CPU's in about 7 hours. However, higher resolution (frequency) requires more powerful computers (i.e. more CPU's).

Note in **Figure 4.8** that the 3D model reproduces the character of the observed waveforms with long duration. The 1D model predicts a very simple, short duration surface waveform. This example illustrates that long-duration surface waveforms can be generated from propagation through the thick sedimentary cover in the Gulf. We propose to investigate long-period ground motions from other events in the Zagros recorded along the Gulf coast by stations operated by the SGS. More recently deployed stations offer a better sampling than the single HASS station provides.

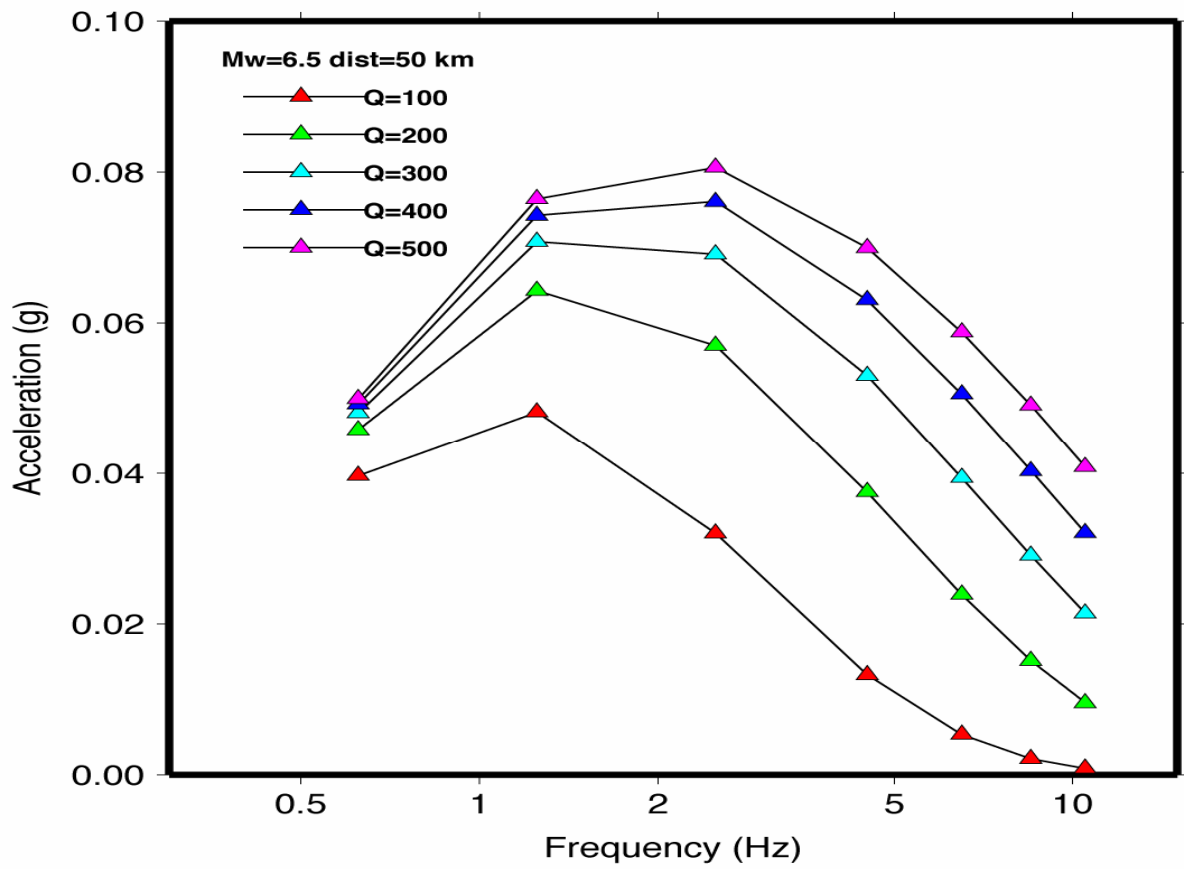
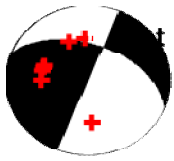
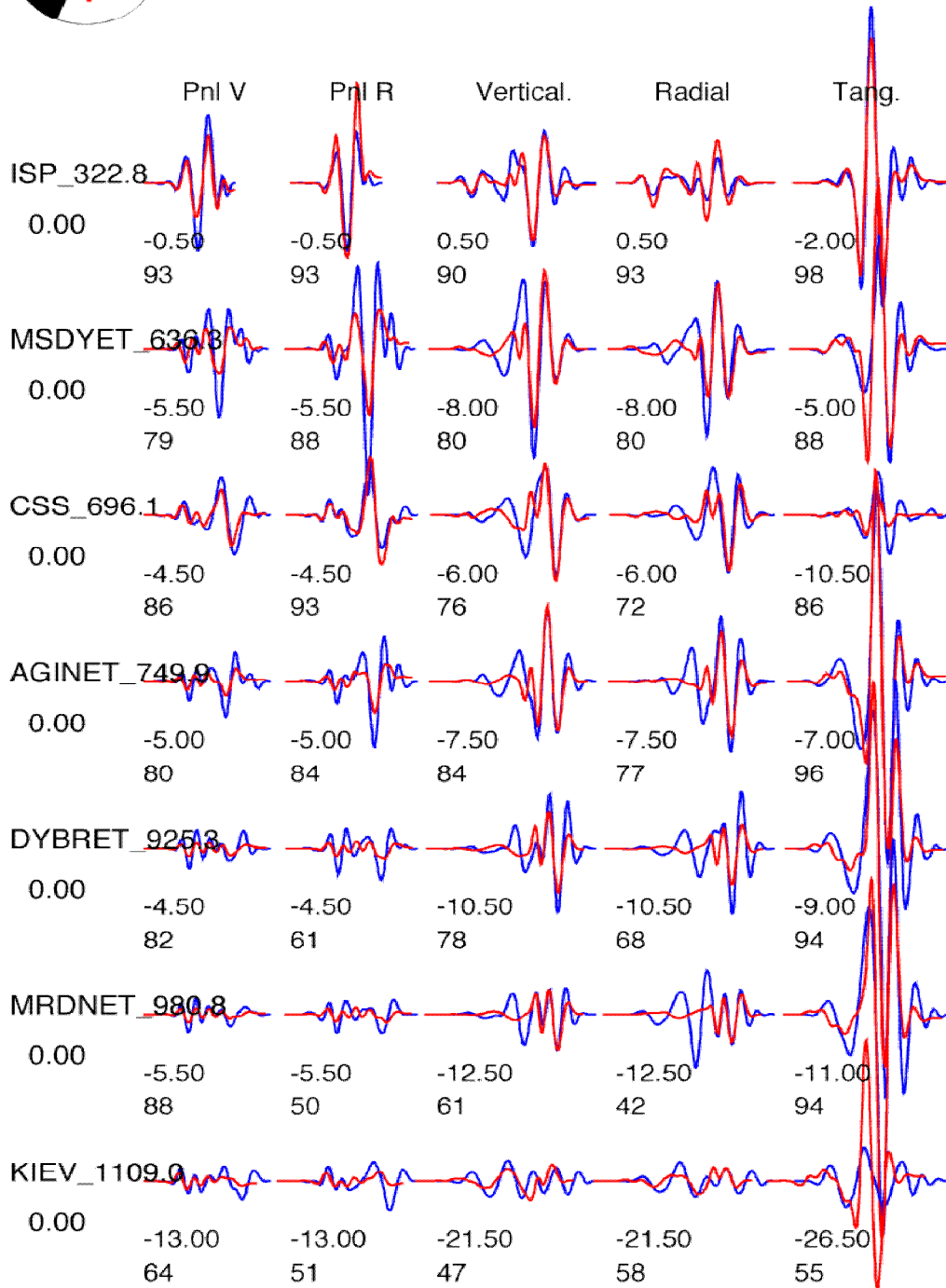
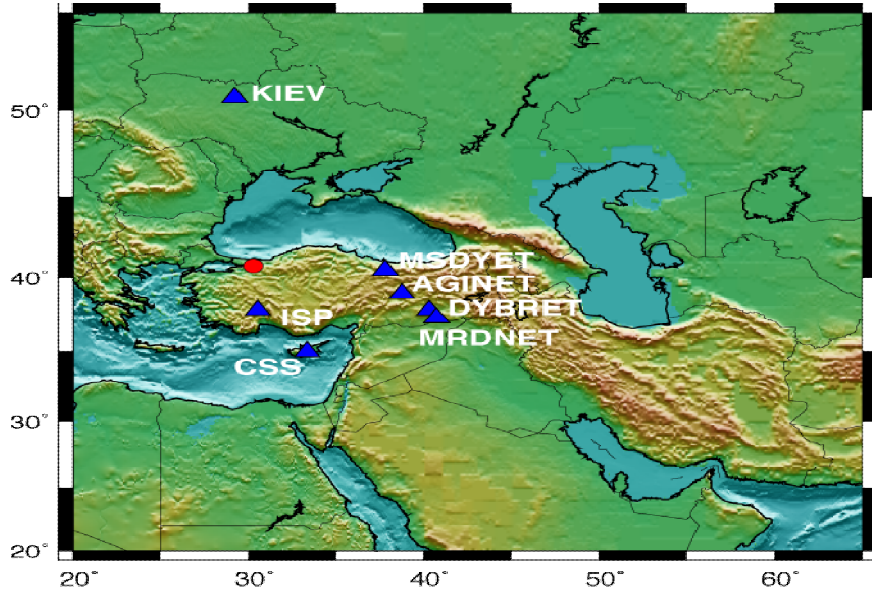


Figure 4.4 Hypothetical spectral accelerations from a Mw 6.5 event at 50 km distance from an observed Lg phase where Q along the path at all frequencies varies from 100 – 500.



t 1321177 Model iran Depth 8 FM 22 90 40 Mw 5.42 rms 2.464e-02





EVID: 1321177
Filters: (Pnl) 0.03 - 0.07 (SW) 0.02 - 0.05
Pnl weight: (Pnl) 2

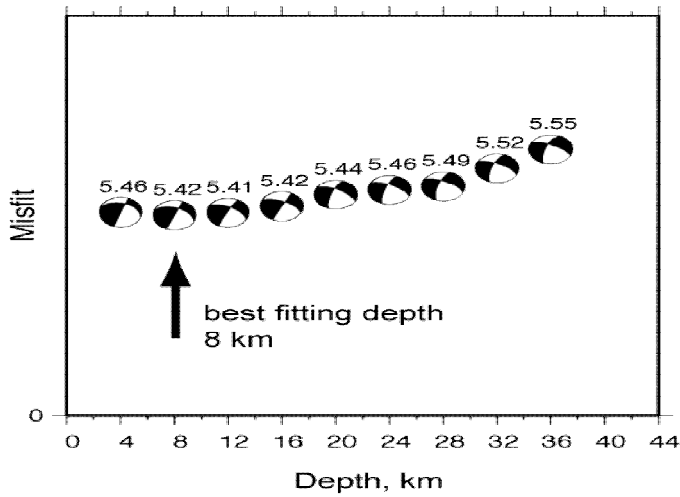


Figure 4.5 Example of waveform fitting for an event in Turkey. The figure shows the observed (blue) and synthetic (red) waveforms segments for the best solution, a map of the event and stations used in the inversion and the depth-mechanism-misfit plot.

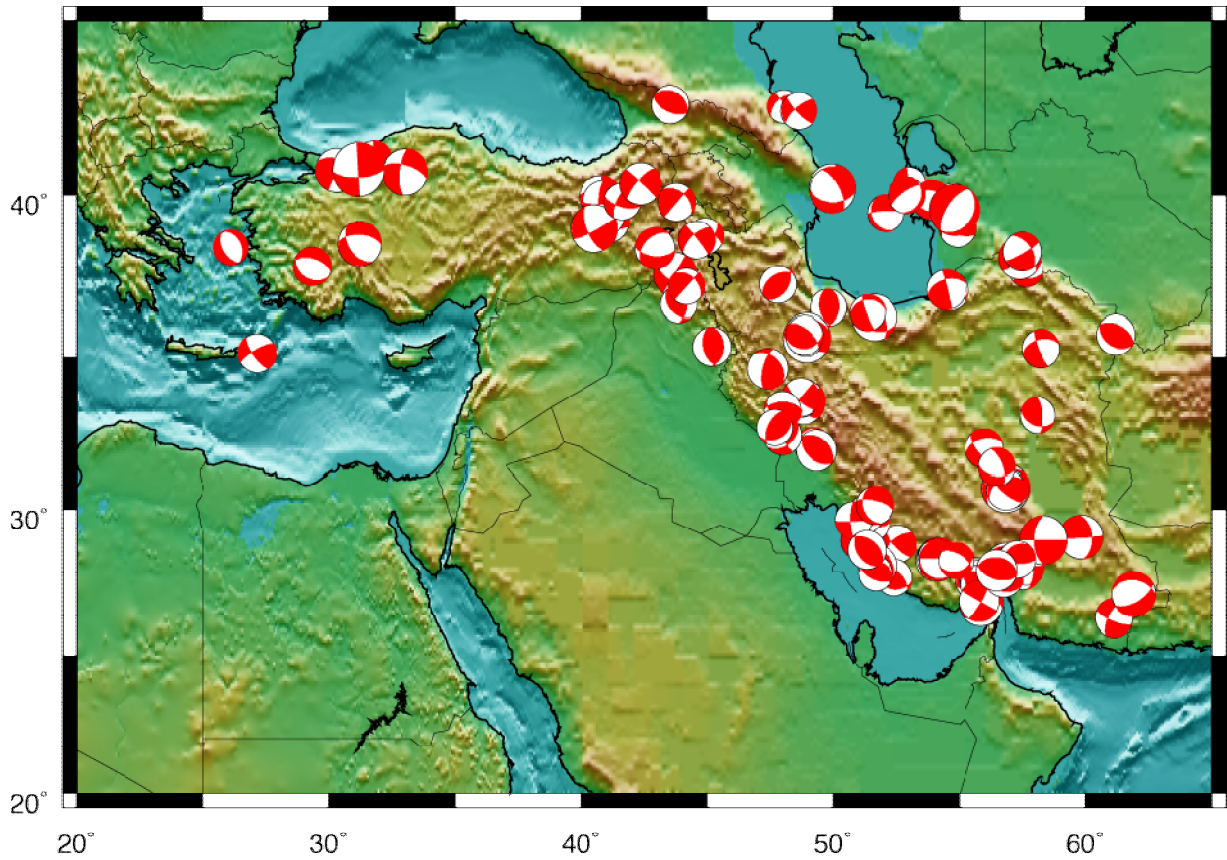


Figure 4.6 Map of events for which we have modeled source parameters in the Turkish-Iranian Plateau. In this project we will develop a catalog of source parameters for events in and around Saudi Arabia.

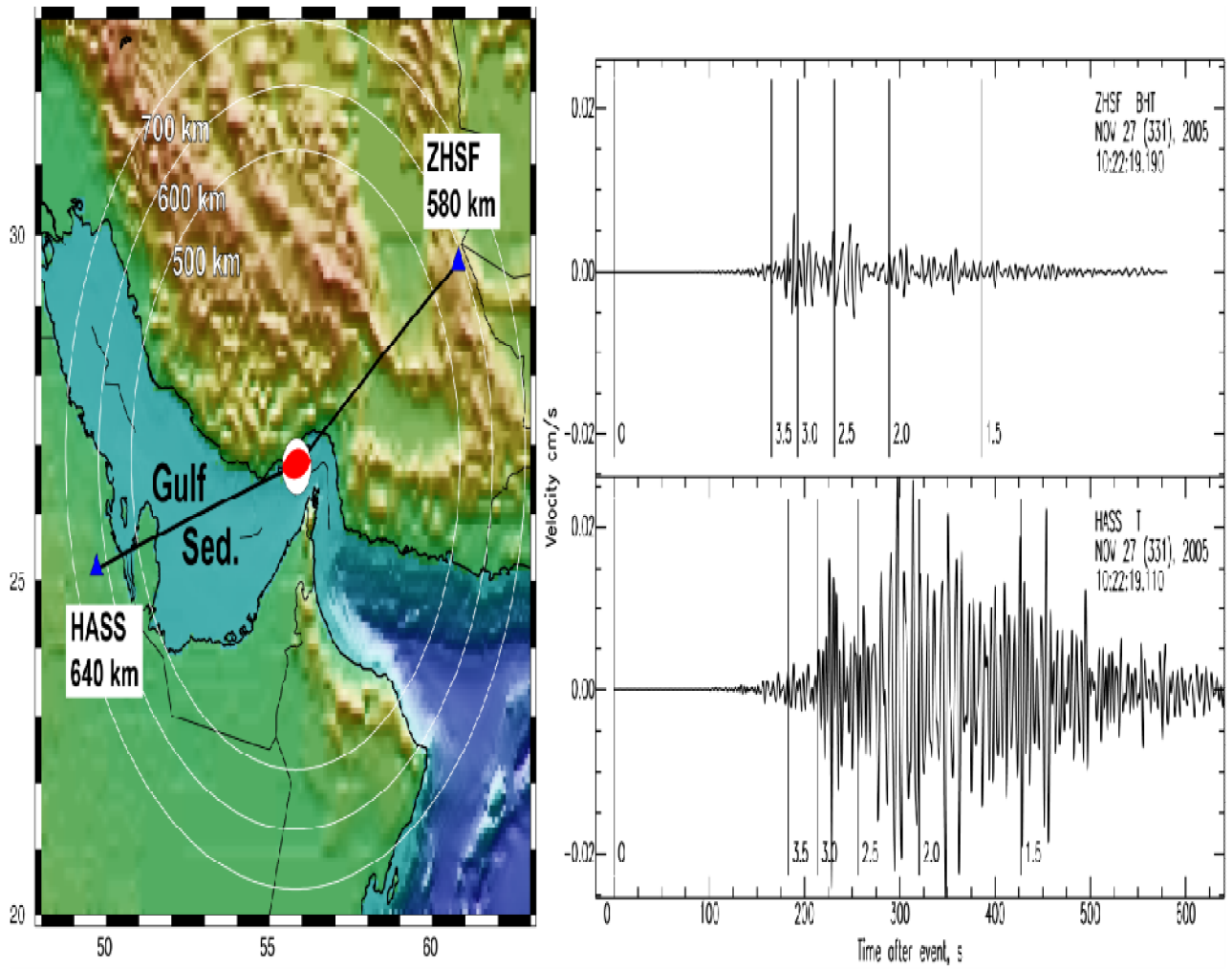


Figure 4.7 (a) Map of the November 27, 2005 Qeshm Island earthquake, focal mechanism and paths to station HASS (Al-Hasa, Eastern Province, Kingdom of Saudi Arabia) and ZHSF (Zahedan, Iran). (b) Transverse component seismograms for the event at ZHSF (top) and HASS (bottom) filtered 0.1–0.3 Hz.

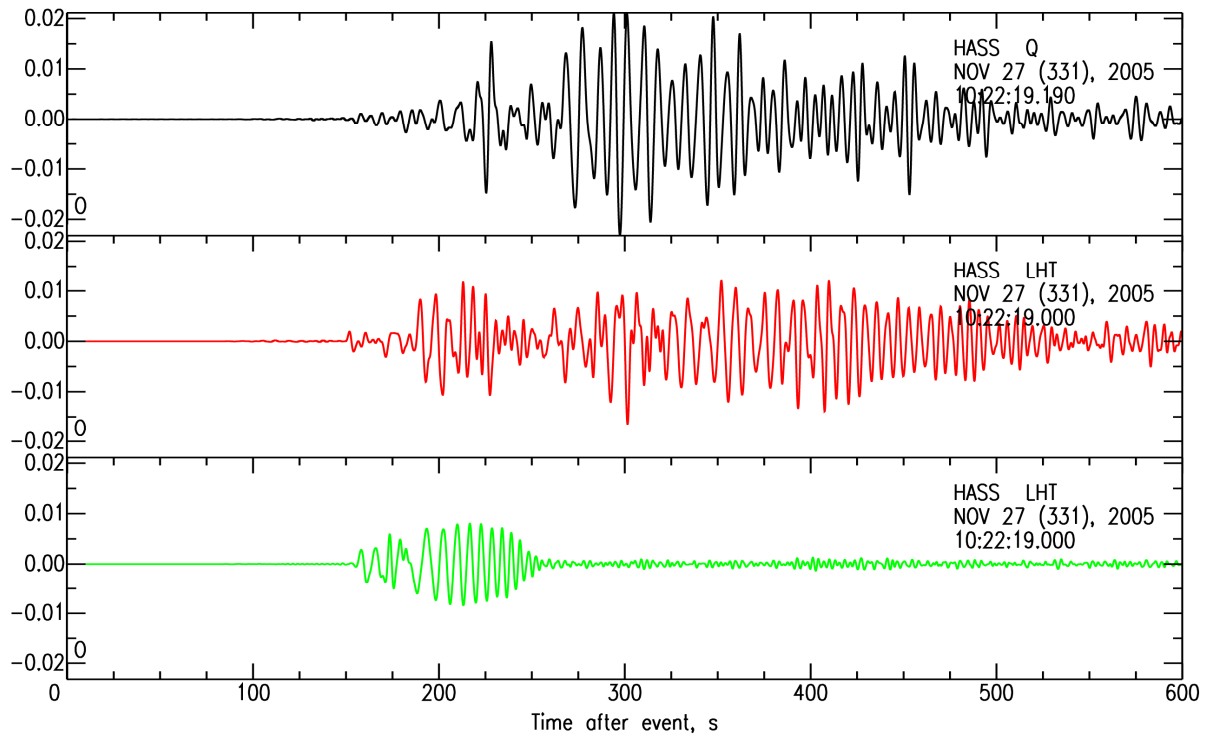


Figure 4.8 (top, black) Observed transverse component ground motion from the Nov. 22, 2005 Qeshm Island event at station HASS (Al-Hasa, eastern Saudi Arabia) along with simulated motions (middle, red) from the CUB2.0 3D model and (bottom, green) iasp91 1D model. Note that the CUB2.0 3D model reproduces the long-duration and better approximates the amplitude than the iasp91 1D model. Note that the data and synthetic seismograms have been filtered between 0.1-0.2 Hz.

5. Results & Data Analysis

5.1 Data Collection

We are interested in recordings of seismic data of stations throughout the Kingdom in order to provide coverage for source parameter determination and amplitude measurements. Events of interest include earthquakes from a wide range of magnitudes (likely M 3.5 – 6.5) and from both within Saudi Arabia and the broader region (**Figure 5.1**).

Co-I Dr. Michael Pasyanos visited Riyadh on April 21-29, 2011. The purpose of his trip was to negotiate with the PI how the project would be achieved and discuss the training mechanism as well as extracting earthquake data for the project which represents an important component to accomplish the work.

Data was obtained for hundreds of regional and teleseismic events recorded at the Saudi National Seismic Network (SNSN), a network of broadband stations covering the kingdom (**Figure 4.3**).

Data was also obtained from the Al-Rayn seismic array (**Figure 5.2**), a rather unique seismic array in the middle of the country (Al-Amri et al., 2012) that is comprised of a central broadband station along with an array of complementary three-component stations (normally arrays have only single component complementary stations). In addition, an extremely large dataset was obtained of recordings of the Harrat Lunayyir volcanic earthquake swarm. In addition, one month of continuous data from the SNSN is provided for noise-correlation work.

5.2 Determine Source Parameters

We estimated source parameters for events in the area by modeling long-period complete regional waveforms. We modeled large well-characterized events to determine optimal seismic wave speed models for the Peninsula, although we have some good estimates from previous studies (e.g. Rodgers et al., 1998; Al-Damegh et al., 2008). Earthquake source

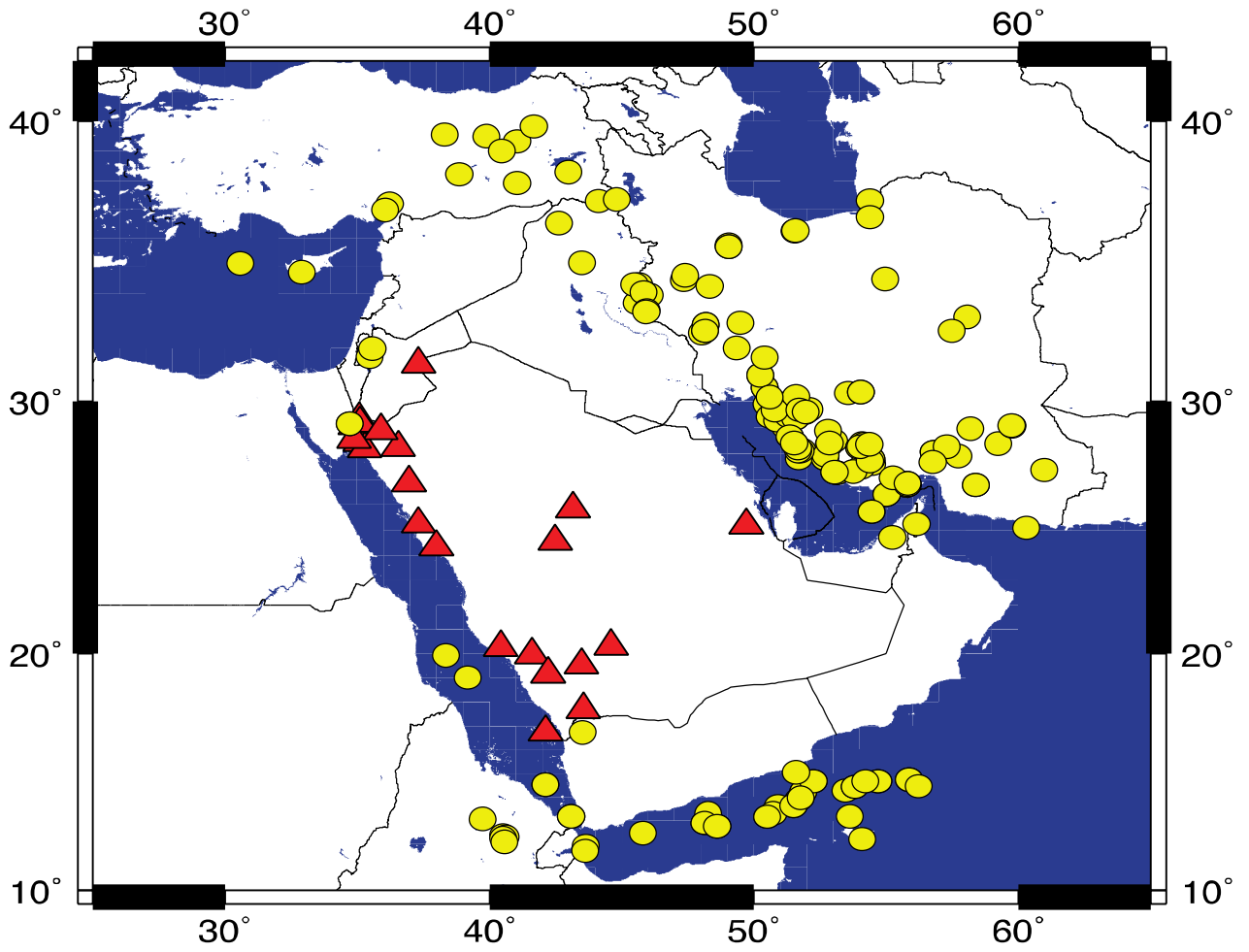


Figure 5.1 SNSN stations (red) and regional earthquakes (yellow) for which we have already made phase amplitude measurements.

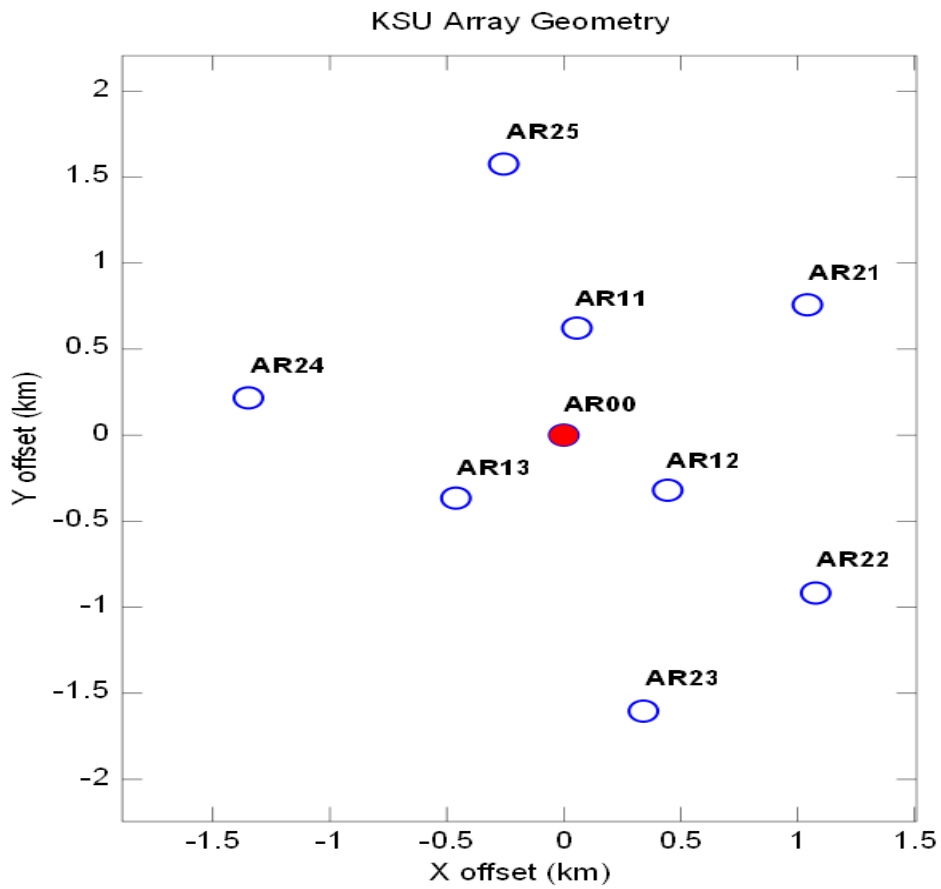


Figure 5.2 The Ar Rayn seismic array has a broadband (STS-2) three-component sensor at its central location(filled circle) surrounded by two rings of three-component short-period (SS-1 Ranger) sensors (Al-Amri et al.,2012).

parameters inform the nature of expected faulting and can be used to predict the range of ground motions for possible future earthquakes. Estimates of seismic moment from these events will be used to populate initial values of the source terms in the attenuation inversion. double-couple focal mechanism by breaking the regional waveform into its constituent segments (Pnl, Rayleigh and Love waves). Doing so allows filtering the Pnl waveform differently from the surface waves and allowing the waveform segments to be advanced or delayed in time independently to account for errors in the assumed plane-layered seismic structure.

We determined the focal mechanisms, depths and moment magnitudes for earthquakes in the Middle East using the “Cut-and-Paste” (CAP) method Zhao and Helmberger (1994) and Zhu and Helmberger (1996). This method modifies conventional grid search approaches for the best.

The CAP method breaks the complete regional waveform into three (3) phases using five (5) constituent segments, specifically the Pnl on the vertical and radial components, the Rayleigh wave on the vertical and radial components and the Love wave on the transverse component. A grid search then systematically tests focal mechanism (i.e. each combination of strike, dip and rake) at a given depth, accumulating the waveform misfit for each mechanism. A library of Green’s functions (GF’s) for an appropriate plane-layered seismic model are pre-computed.

Figure 5.3 shows an example event in the Zagros Mts. in SW Iran recorded at stations in Saudi Arabia and Kuwait. The event was determined to have a depth of 8 km, a moment magnitude of 4.15, and a thrust mechanism that is consistent with faulting in the region. Focal mechanisms from regional broadband waveforms in the Middle East illustrate the complexity of active tectonics in the region (**Figure 5.4**). Specifically we report a variety of faulting across the region. We observed strike-slip motion on the North and East Anatolian Faults and normal

faulting in western Anatolia. The Arabian-Eurasian collision reveals mostly low-angle thrust faulting along the Bitlis-Zagros Thrust belt, with a mixture of strike-slip and rotated thrust events. The initial focus has been on large regional earthquakes, most occurring in the Zagros and eastern Turkey.

Resulting tomographic image of 20 second Rayleigh wave group velocities shows slower than average velocities for the Arabian Platform and Rub Al-Khali, probably due to low-velocity sediment cover. The Red Sea is faster than average due to thinner crust. The 20 second group velocities gradually increase from the Eastern Province to the Hejaz and Red Sea. The inclusion of additional surface wave dispersion data could help resolve three-dimensional structure of Saudi Arabia.

5.3 Measure Regional Phase Amplitudes

We have measured data from over a hundred regional events recorded at the SNSN. These events span a range of magnitudes (from M 3.5 – 6.5) in the region surrounding Saudi Arabia. Pn, Pg, Sn, and Lg phases have currently been identified and measured at 22 SNSN stations. Amplitudes for these phases have been measured in the 0.5-1, 1-2, 2-4, 4-6, 6-8, 8-10, and 10-12 Hz pass bands.

Event 1582024 Model iran Depth 8 FM 111 68 80 Mw 5.14 rms 6.234e-04

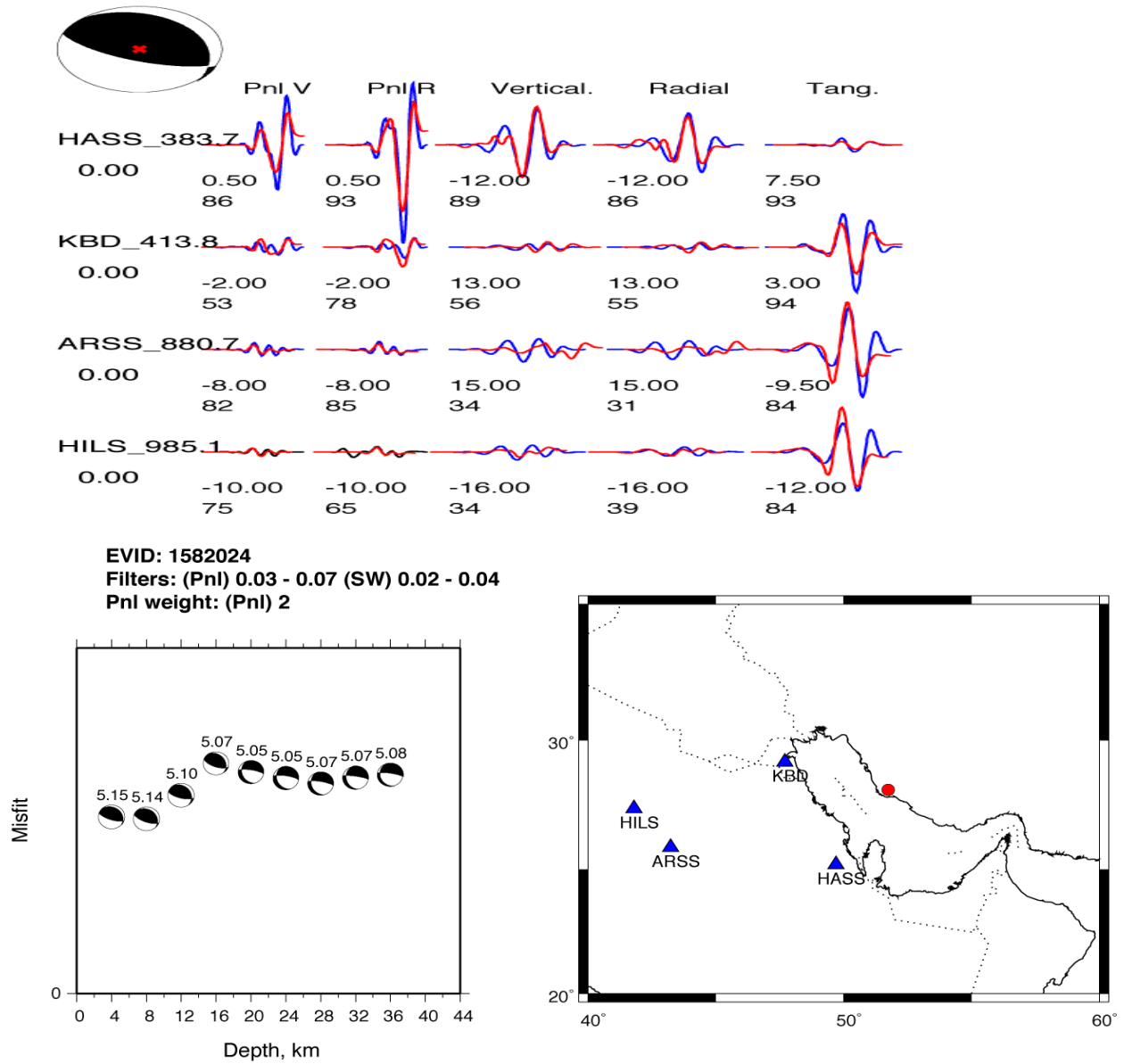


Figure 5.3 Top, left panel shows misfit, moment tensor solution, and moment magnitude as a function of depth. Top, right panel shows location of event (red circle) and stations (blue triangles). Bottom panel shows fit of data (blue) to synthetics (red) for Pnl vertical, Pnl radial, and vertical, radial and tangential surface waves.

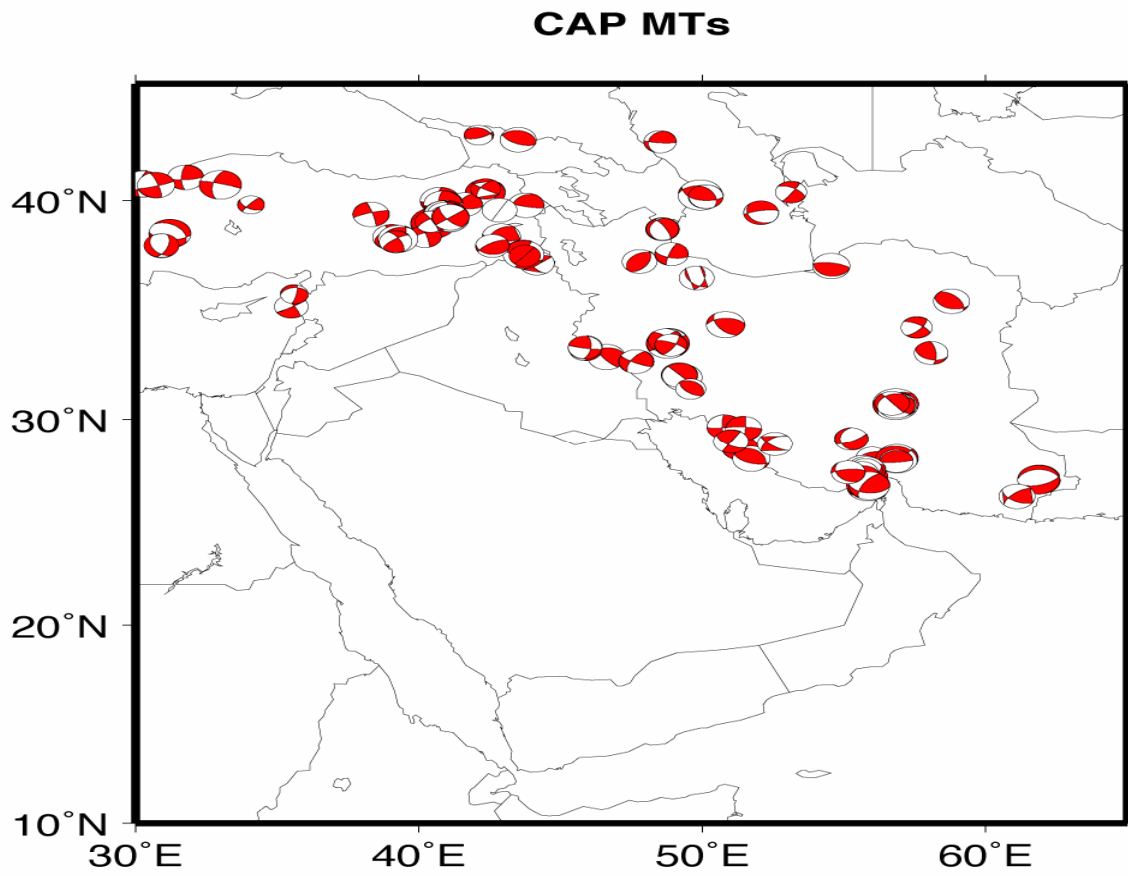


Figure 5.4 Map of regional moment tensor solutions determined using the Cut-and-Paste method.

5.4 Tomographic Imaging for 2D Velocity and Attenuation Maps

Surface wave dispersion measurements are used to create updated Rayleigh and Love wave group velocity maps which have high-resolution over a wide period band. The amplitude measurements can be used in a tomography for surface wave attenuation. In general, surface wave amplitude measurements are more difficult to make than group velocity dispersion measurements because information about the source amplitude is needed, requiring a moment tensor solution. Having a focal mechanism is also needed to avoid making measurements at radiation nodes, where amplitudes can be contaminated by multi-pathing.

We are incorporating the amplitudes measured above into a four-phase attenuation tomography of amplitudes using the method described above. Surface waveform data have already been included in the current tomography (**Figures 5.5 and 5.6**). Input data for the four-phase inversion will be the amplitude measurements from Task 2.1 and the source terms from Task 1.2. Velocity profiles from the source parameter estimation will be used in the inversion. Amplitudes were used to solve for attenuation surfaces (Q_p and Q_s in the crust; Q_p and Q_s in the upper mantle), event source terms, and station site terms. In the process, we modeled the 1D average amplitude attenuation of the region. The attenuation maps were compared and contrasted with our dispersion maps and analyzed for information about the attenuation properties of the sediments, crystalline crust, and upper mantle of the Arabian Peninsula.

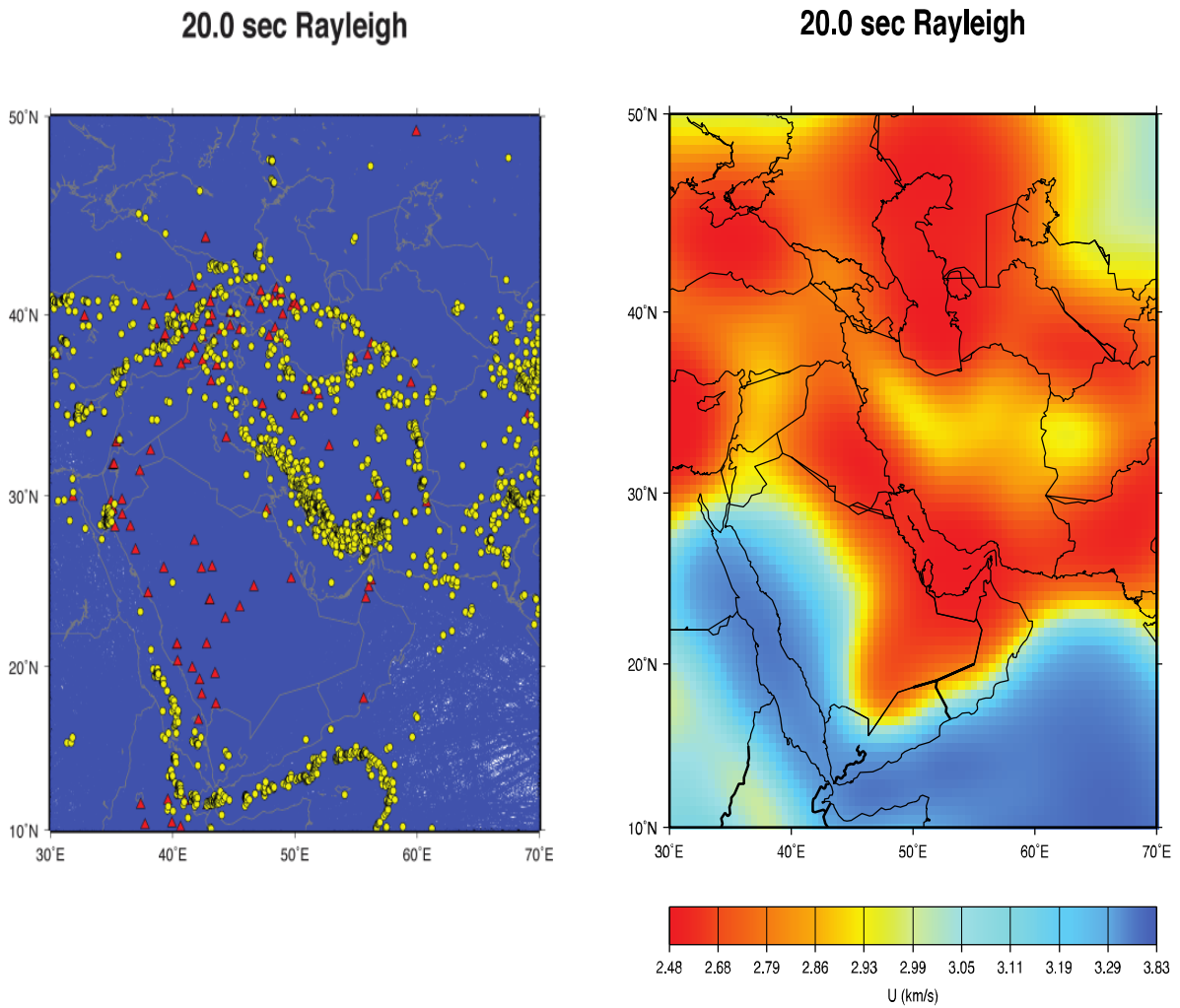


Figure 5.5 Surface Wave Dispersion: (left) path map including regional stations (red) and earthquakes (yellow) used for a tomographic inversion (right) of the Rayleigh wave dispersion data at 20 seconds period. These data have sensitivity to increasingly deeper structure with longer periods (i.e. 15 sec maps with sediments, 50 sec maps with crustal thickness, etc.).

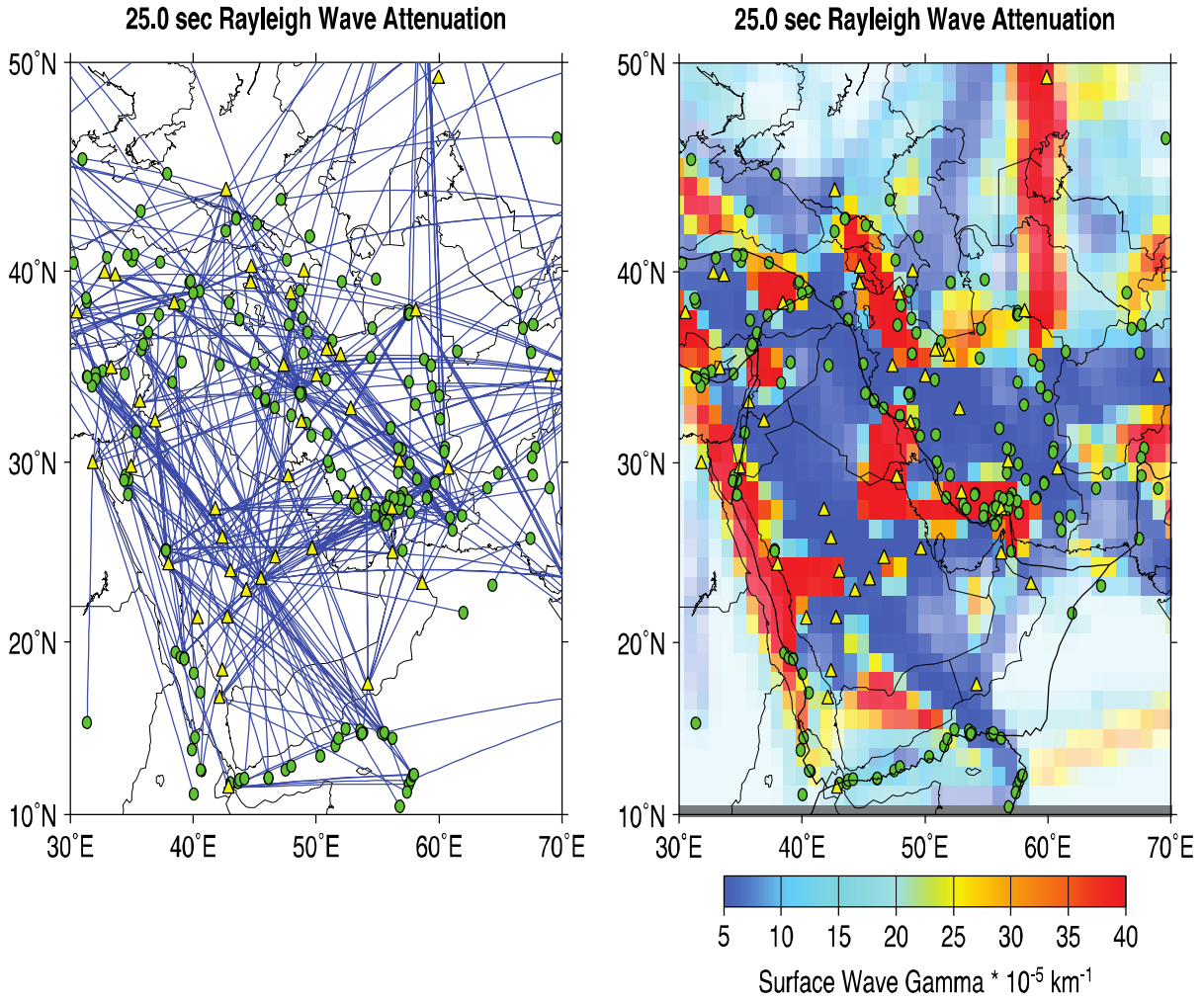


Figure 5.6 Surface Wave Attenuation: Path map (left) and initial result (right) for a surface wave inversion of the 25 second period Rayleigh wave. In these preliminary inversions, we show the attenuation parameter γ where $\gamma = p/UTQ$.

6. Discussion & Interpretation

6.1 Interpreted Seismicity of the Gulf Region

The seismicity map of the Arabian Platform for the period from 1980 to 2010 for magnitude 3 and above is shown in **Figure 6.1** which indicates a sparse distribution of seismic events in the Arabian Platform and western portion of the Arabian Craton. At the central portion of the Arabian shelf, three earthquake events are shown to be positioned among the great anticlines (Summan platform, Khurais-Burgan and Ghawar-En Nala anticlines, Qatar arch) that are bounded by the Wadi Batin and Abu Jifan faults. In the Arabian gulf from the Hormuz salt basin up to the Mesopotamian foredeep of southern Iraq shows also sparse distribution of epicenters, Southeastward of the Arabian shield and south of the central part of the Arabian shelf, three seismic event have epicenters in the Rub Al-Khali basin and two more in the Hadramaut arches in eastern Yemen.

In Oman, two seismic events are located in the Hawasina thrust sheet, while the others are along the Dibba fault and the Makran-Zagros subduction zone. This subduction zone is the only region where an oceanic lithosphere is being subducted, where apparently the oceanic crust in the gulf of Oman is being consumed beneath southern Iran. To the southeast of Oman, along the Masirah trough zone gives one earthquake event. Down south, a spatial concentration of seismic events can be seen. This distribution is in the East Sheba ridge which is between the Alulak-Fartak trench in eastern Yemen to the west and the Owen fracture zone to the east. The ridge is also between the Socotra island in the south and the Masirah trough in the north. The ridge is part of a line of epicenters that connects the gulf of Aden to the west and the Carlsberge ridge to the

south.

However, there is an increasing concentration of earthquake epicenters going toward the northeast directions of the Arabian platform and the zone of convergence below the southwestern direction of Lut block in Iran and parallel to the Oman line. One of the concentrated spatial distribution of seismic events is shown to occur in the Zagros Mountains folded belt that extends for a distance of about 1500 km in a northwest-southeast direction. The simple folded belt is an area of about 250 km in width. The earthquakes in the Zagros folded belt define a zone of about 200 km wide that runs parallel to the fold belt. The majority of earthquakes occur in the crustal part of the Arabian plate that is subducted along the folded belt. Magnitude 5 earthquakes are frequent and magnitude 6 may occur sometimes yearly. This tendency of increasing seismicity thins out in the Main Zagros Thrust (MZT) and the Sanandaj-Sirjan ranges in Iran. The nature of deformation across this zone is complex, involving both thrust and strike-slip as indicated by earthquake focal mechanisms (Telebani and Jackson, 2004).

To the west to the Musandam Peninsula, Arabia is under thrusting the southern Eurasian margin along the Zagros Thrust. To the east of the Musandam Peninsula, convergence is much slower given the seismicity along the Makran coast. Strike-slip motion probably occurs along reactivated thrust planes associated with obduction of the Semail Ophiolite (Oman Mountains). The Makran subduction is the region where the Gulf of Oman is continue to subduct under the southern region of the Eurasian plate. It differs from other subducting segments of the Arabian Plate in that it is an oceanic crust rather than continental crust that is being subducted beneath Eurasian Plate. This oceanic crust extends eastward to Owen Fracture Zone (OFZ) along the Indian Plate boundary.

A moderate ($M \sim 5$) earthquake struck the town of Masafi in the northeastern UAE on March 11, 2002 (**Figure 6.1**). The event was large enough to be detected and located by global networks at teleseismic distances. The region is generally believed to be aseismic, however no regional seismic network exists in the UAE to determine earthquake occurrence.

Accordingly, twelve seismogenic source zones were delineated and identified based on seismological and geological parameters with the higher priority given to the spatial distribution of epicenters. These source zones are composed of systems of faults whose boundaries do not traverse generally other tectonic units. Some of the seismogenic source zones are relatively large due to scarcity of earthquakes in the Arabian Platform (Alamri, 2013).

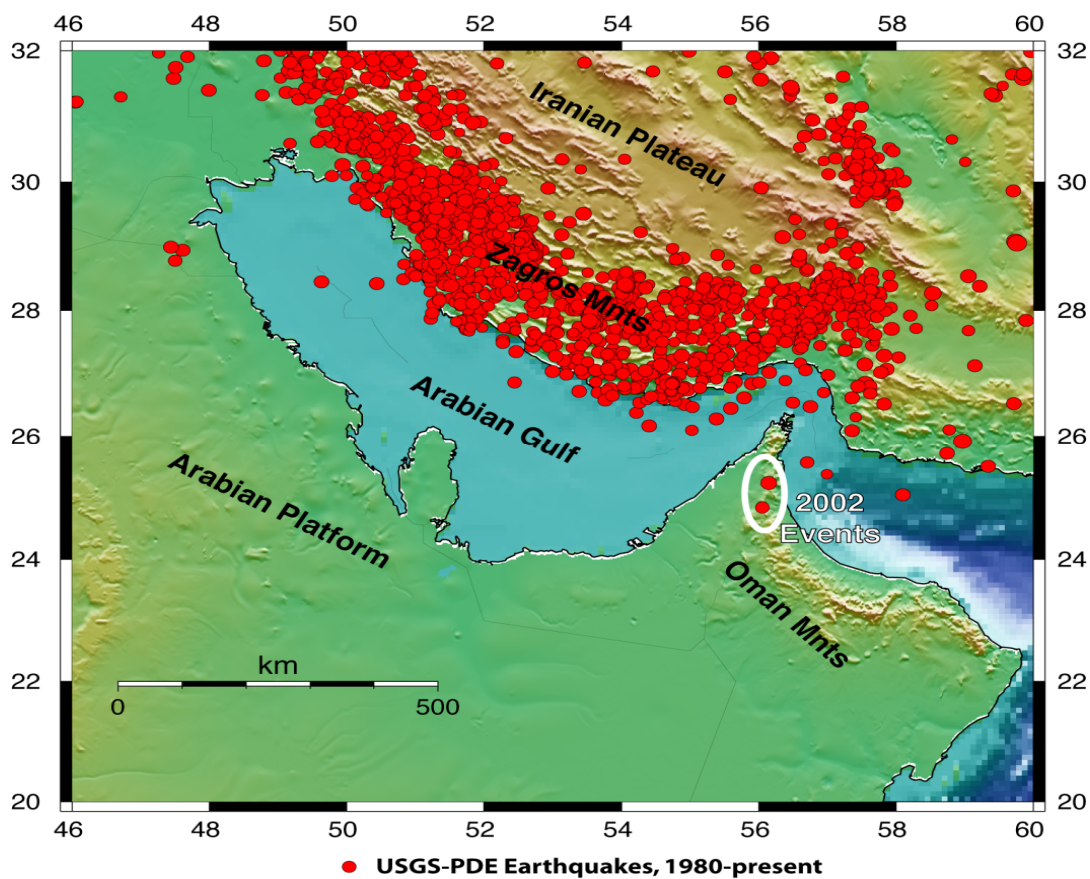


Figure 6.1 Seismicity of the Arabian Platform and adjacent regions (1980 - 2010).

6.2 Analysis of Long -Period Ground Motions in the Gulf

The Arabian Gulf is adjacent to one of the most seismically active fold-and-thrust belts on Earth, the Zagros Mountains. Broadband seismic records of earthquakes in the Zagros Mountains recorded on the Arabian side of the Gulf display long duration surface waves. While shorter periods (< 1 s) are attenuated from crossing the deep sediments (> 10 km) of the Gulf basin, the long period energy is relatively unaffected. Consequently large earthquakes in the Zagros could result in possibly damaging ground motions at long-periods (1-10 s). Such ground motions are of concern for large engineered structures, such as tall buildings and long bridges with resonant periods in the same frequency band (period of 1-10 s). Basin structure of particular concern for earthquake hazard in the Gulf. Several large earthquakes in the Zagros have resulted in felt ground motions along the western coast of the Gulf.

In a recent study we demonstrated that the sedimentary geology of the Arabian Gulf causes higher amplitude and longer duration ground shaking than would be expected in more normal continental crustal structure. The most seismically active region near the Kingdom of Saudi Arabia is the Zagros Thrust Belt. Large ($M > 6.0$) events occur on average at least once a year or more frequently in this region; however, these events are 200 km or greater from the Arabian coast. Ground motion hazard for such large distances is unusual. Nonetheless, ground motions caused by distant events in the Zagros have resulted in felt motions in tall buildings in cities along the Arabian coast. An example of this is the November 22, 2005 M 5.7 Qeshm Island. This event caused motions in tall buildings in Dubai, United Arab Emirates, and other cities along the Gulf coast. The locations of earthquakes and seismic stations considered in this study are shown in **Figure 6.2**.

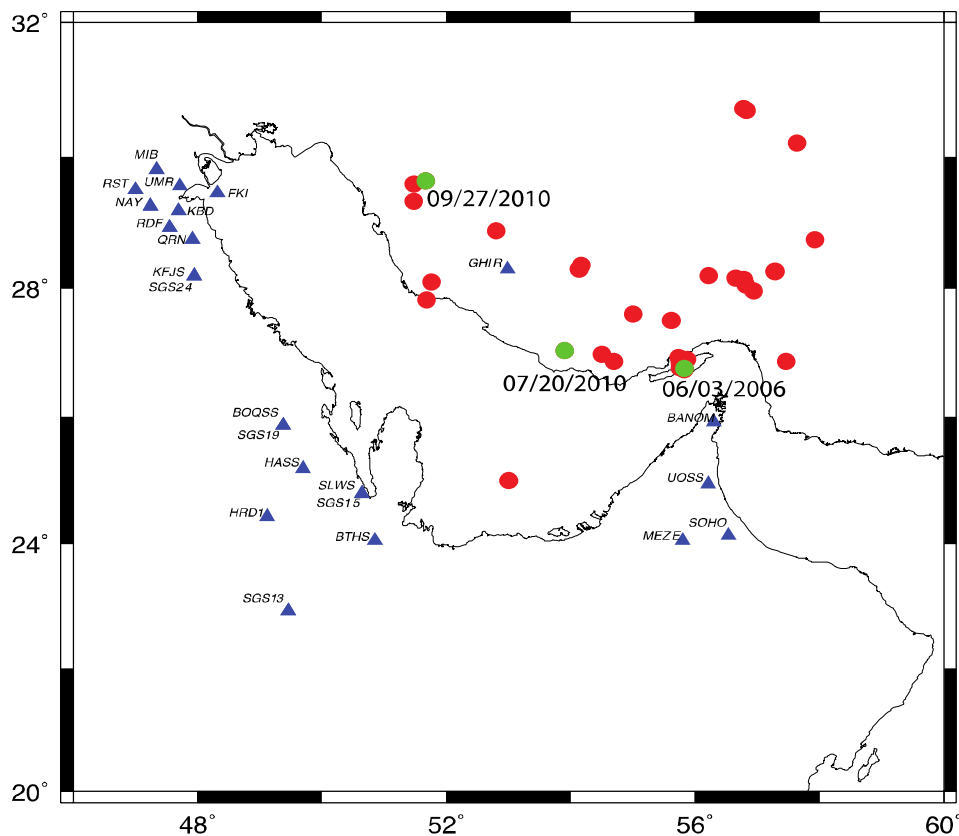


Figure 6.2 Map of study area showing earthquakes (circles) and seismic stations (triangles). Green circles show the location of three earthquakes considered in the comparisons of acceleration response spectra shown in **Figure 6.7**.

As mentioned earlier, the Arabian Gulf is composed of a deep sedimentary basin. Sediments of the Arabian Platform dip eastward, reaching a depth of up to 10 km adjacent to the Zagros. **Figure 6.3** shows a map of depth to basement in the region. The deep structure of the Gulf is composed of geologically old and consolidated sediments with moderately high shear velocities (Pasyanos et al., 2012). However, the younger sediments near surface have much lower velocities and probably low attenuation. The Moho discontinuity beneath the western Arabian Platform indicates a velocity of 8.2 km/sec of the upper mantle and 42 km depth (Al-Amri, 1998; 1999). The sedimentary sequence covering most of the Arabian platform has an

average thickness of 5 km and its shear velocity is 2.31 km/s. Its thickness increases towards the east under the interior platform and basins, where it is 7 km on average and consists of two layers-an upper 3 km with a shear velocity of 2 km /s and a lower 4 km with a shear velocity of 3.24 km/ s. Seismic velocities within the Gulf sediment structure are very low. Basin structure “traps” and “amplifies” seismic waves. Near-surface (< 50 m) velocities most strongly control ground motions amplitudes.

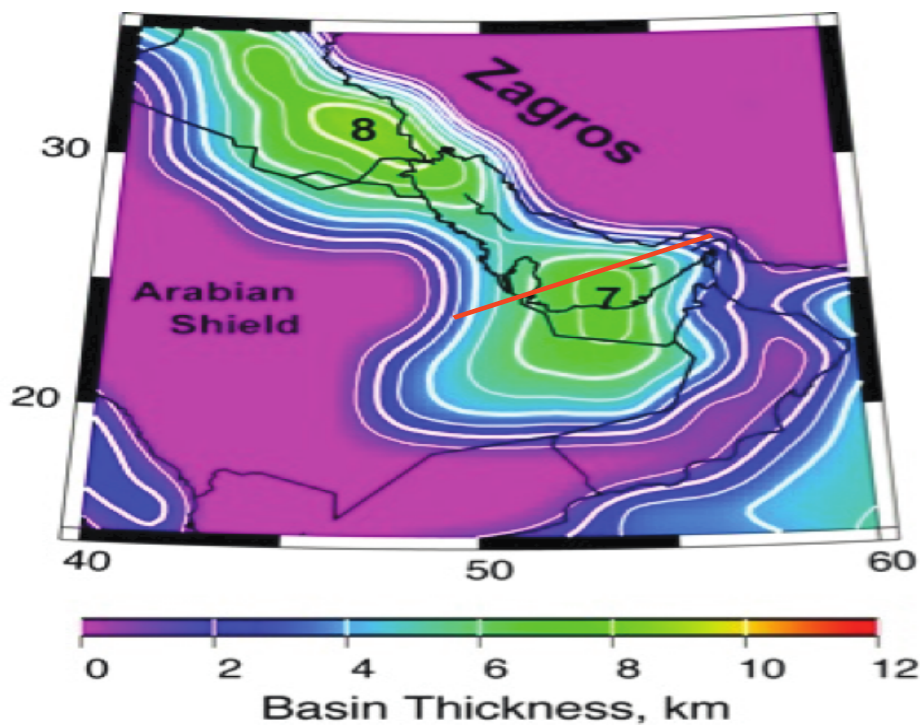


Figure 6.3 Sediment thickness of the Arabian Gulf and surrounding region. Red lines indicates the location of the cross section of the basin used in simulating basin structure effects.

This complex basin structure is of particular concern for earthquake hazard in the Gulf. Several large earthquakes in the Zagros have resulted in felt ground motions along the western coast of the Gulf. These events have been particularly strongly felt in high-rise buildings in the urban centers along the Gulf, such as Ad Dammam (Saudi Arabia), Kuwait City (Kuwait), Doha

(Qatar), Abu Dhabi, Dubai and Sharjah (UAE). This task seeks to provide a quantitative measurement of these ground motions using broadband seismic records. In particular, this project is concerned with long-period (1-10 seconds) ground motions observed in the western side of the Arabian Gulf from earthquakes in the Zagros Mountains and Iranian Plateau to the east of the Gulf.

Ground motion recorded at seismic stations in eastern Saudi Arabia from the M 5.1 June 3, 2006 earthquake, located near Qeshm Island, were selected to illustrate this phenomenon (**Figure 6.4**). The seismic response (north component, corresponding most naturally with the transverse component) is shown for two frequency (period) ranges: (a) 0.02-0.05 Hz (50-20 seconds) and 0.1-1.0 Hz (10-1 seconds). The longer period band (50-20 s) shows the surface waves arriving between 3.5 and 3.0 km/s, as expected for normal continental paths at regional distance. The surface wave is relative simple without an unusually long duration and is normally dispersed as expected. However, at the shorter period the response shows an unexpectedly long duration of up to hundreds of seconds and at lower group velocities of 3.0 – 1.5 km/s. This long duration shaking in the period band 1-10 seconds will cause increased loading on large engineered structures with sensitivity to this band. Similar observations have been made for other earthquakes recorded at station HASS for which the wave path goes through the thick sedimentary cover in the Arabian Gulf.

The observed extraordinarily long duration are likely due to a waveguide effect from the deep sedimentary structure which enhances long-period ground motion (e.g. Mellors et al., 1999). Strictly speaking these motions are short-period surface waves, but longer-period ground motion, which is normally observed, is of concern for seismic hazard. This period range is of importance

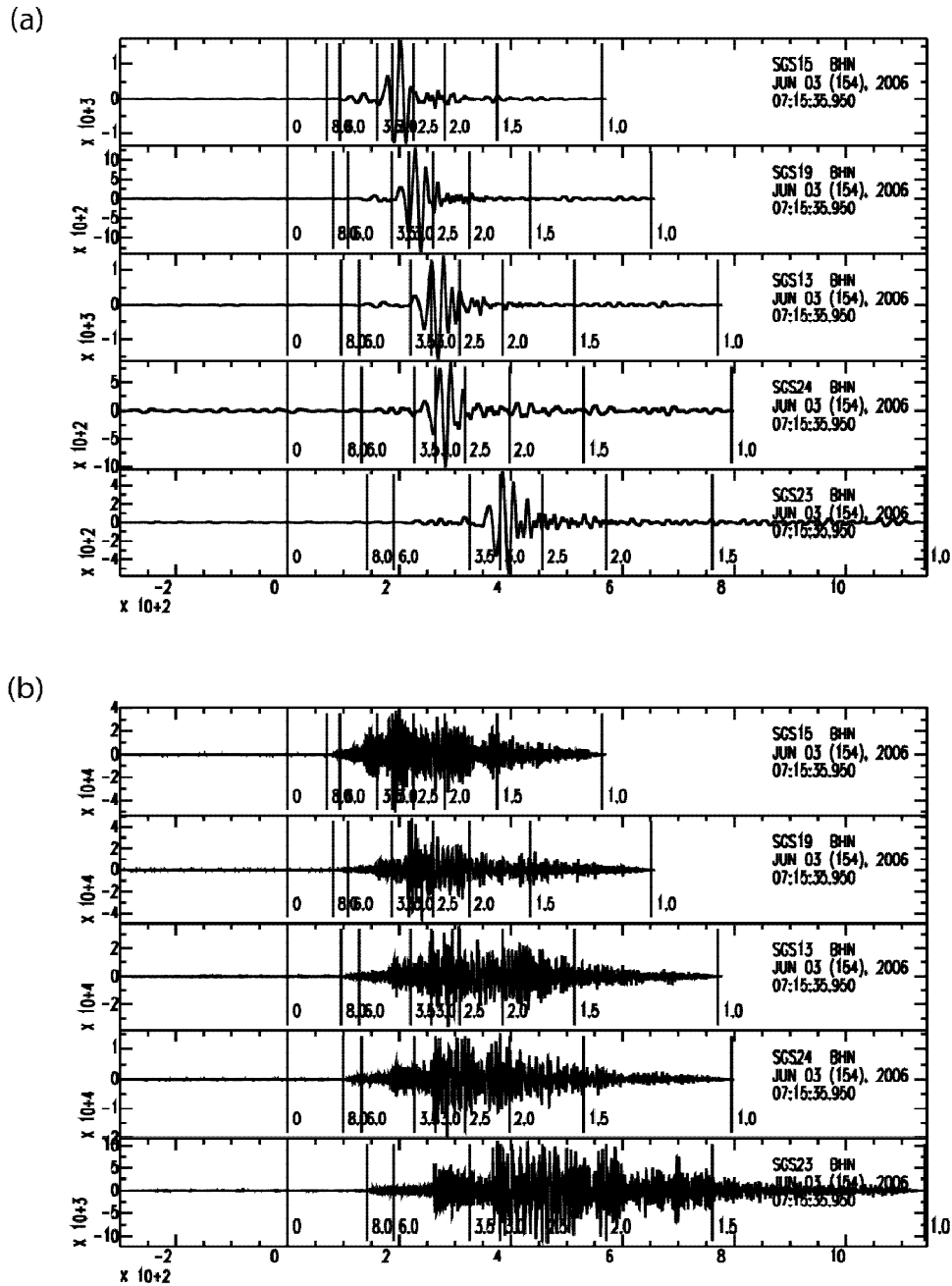


Figure 6.4 Seismograms for 3 June, 2006 earthquake recorded at stations in eastern Saudi Arabia filtered (a) 0.02-0.05 Hz (50-20 seconds) and (b) 0.1-1.0 Hz (10-1 seconds). Each plot includes the group velocities in km/s. Note that the 10-1 second period band shows an usually long duration signal of more than 200 seconds in the group velocity window 3.0-1.5 km/s.

for evaluating earthquake ground motion hazards for large engineered structures with natural periods in the range 1-10 seconds, such as tall buildings, long bridges, and pipelines.

Seismic waveforms are affected by both path and source effects (e.g., Pitarka et al., 1998). Path effects are caused by varying material properties along the wave path. Differences in wave path for different source locations and depths cause variations in amplitude and duration, and are usually frequency dependent. Lateral and vertical variations in velocity cause dispersion, diffraction, and reflections, all of which affect wave amplitude and duration. The effect of wave scattering is significant at intermediate frequencies (0.05-1 Hz) as the waves propagate in the top sedimentary layers of the Gulf and eastern Arabian platform. Attenuation, which tends to affect higher frequencies more than lower frequencies, often is stronger in sedimentary basins than in older shield areas. Increased duration and relatively large amplitude of ground motion recorded along the western side of the Gulf region suggests that seismic attenuation is very low. The earthquake source itself varies both in focal mechanism and in depth, which also affects ground motion characteristics at all distances. Long-period ground motions are more likely to impact large structures because the resonant period of large structures is longer than small structures. It is the purpose of this report to investigate and understand the causes of these extraordinarily long duration surface waves for paths crossing the Arabian Gulf.

6.3 Recorded Spectral Response Characteristics

An effective tool in analyzing multiple seismic records of ground motion and their potential effects on buildings is the acceleration response spectrum. Here we show the spectral response at various locations as compared with two empirically derived ground motion prediction equations (GMPE): Campbell and Bozorgnia (2008) and Boore and Atkinson (2006), hereafter referred as

CB08 and BA06. These equations are based on regressions of ground motion data from selected earthquakes around the world. They should be distinguished from the simulation-based models presented in Task 4. CB08 equation, a Next-Generation Attenuation (NGA) equation, was designed for active shallow crustal structures. It is controlled by various parameters, including earthquake magnitude, distance, type of rupture, and basin depth (depth to layer with $V_s=2.5$ km/s). Importantly, basin effects, as might be expected in the Gulf, are included. Because of the limited amount of good quality data the standard deviation of this equation is large at distances longer than 200km and periods shorter than 3s. On the other hand AB06 is better constraint at large distances. It is developed for eastern North America, which in some respects resembles the sediments/shield structure of eastern Arabian Platform.

We compared the recorded spectral response with the two GMPEs. **Figure 6.5** shows the spectral acceleration ratios of recorded and predicted ground motion using CB08 for the geometric mean horizontal component at periods 1s, 5s, and 10s, and 5% damping. The predicted ground motion was computed for a depth to basement of 3.5 km. The recorded motion is much higher than the one predicted by the GMPE at the period of 10 s. It is comparable at the 5 s period and much lower at the 1 s period. **Figure 6.6** shows the mean spectral acceleration ratios of recorded and predicted ground motion at periods 1s, 5s, and 5% damping computed using BA06. The comparison with both GMPEs clearly shows that due to basin effects the ground motion is amplified significantly at periods 5s and 10s. In contrast the ground motion is reduced significantly at 1s periods.

Figure 6.7 illustrates the ground motion amplification along different wave paths, across the Gulf basin, for three earthquakes. We used recorded acceleration response spectra from the M5.3, 2006/06/03 earthquake, M5.7, 2010/07/20 earthquake, and M5.9, 2010/09/27 earthquake,

at stations with good quality data in the Arabian Gulf region. When looking at the response spectra from the 2010/09/27 earthquake, the most striking feature is the difference in spectral amplitudes in the E-W component between station SGS15 and the rest of the stations. At SGS15 the E-W spectral acceleration is much larger in the period range 0.5-4 s. In contrast, the spectral amplitudes at station SGS19, which has similar epicentral distance but located further to the north, are similar to those recorded by the other stations. The observed differences between SGS15 and SGS19 is a clear indication of very different wave propagation effects along paths across the basin. A similar trend is seen for the 2010/07/20 event located in the center of the Gulf region. Although the epicentral distance of SLWS is twice as large as that of UOSS the observed spectrum at this station is at least a factor of 10 larger especially in the period range of 1-10 s. The two stations stand on opposite wave paths with very different basin depths. UOSS located in the shallow part of the basin has a flat spectrum, whereas at SLWS the spectral amplitudes peak in the period range of 2 -8 s. Very similar spectral characteristics, apparently caused basin surface waves, are seen in the other two stations.

Based on these observations, we concluded that the deep sedimentary structure in the Gulf acts as a wave guide that enhances seismic wave amplification along paths that cross the basin. Therefore, the knowledge of the basin structure is crucial in predicting strong ground motion in the western coast of the Gulf.

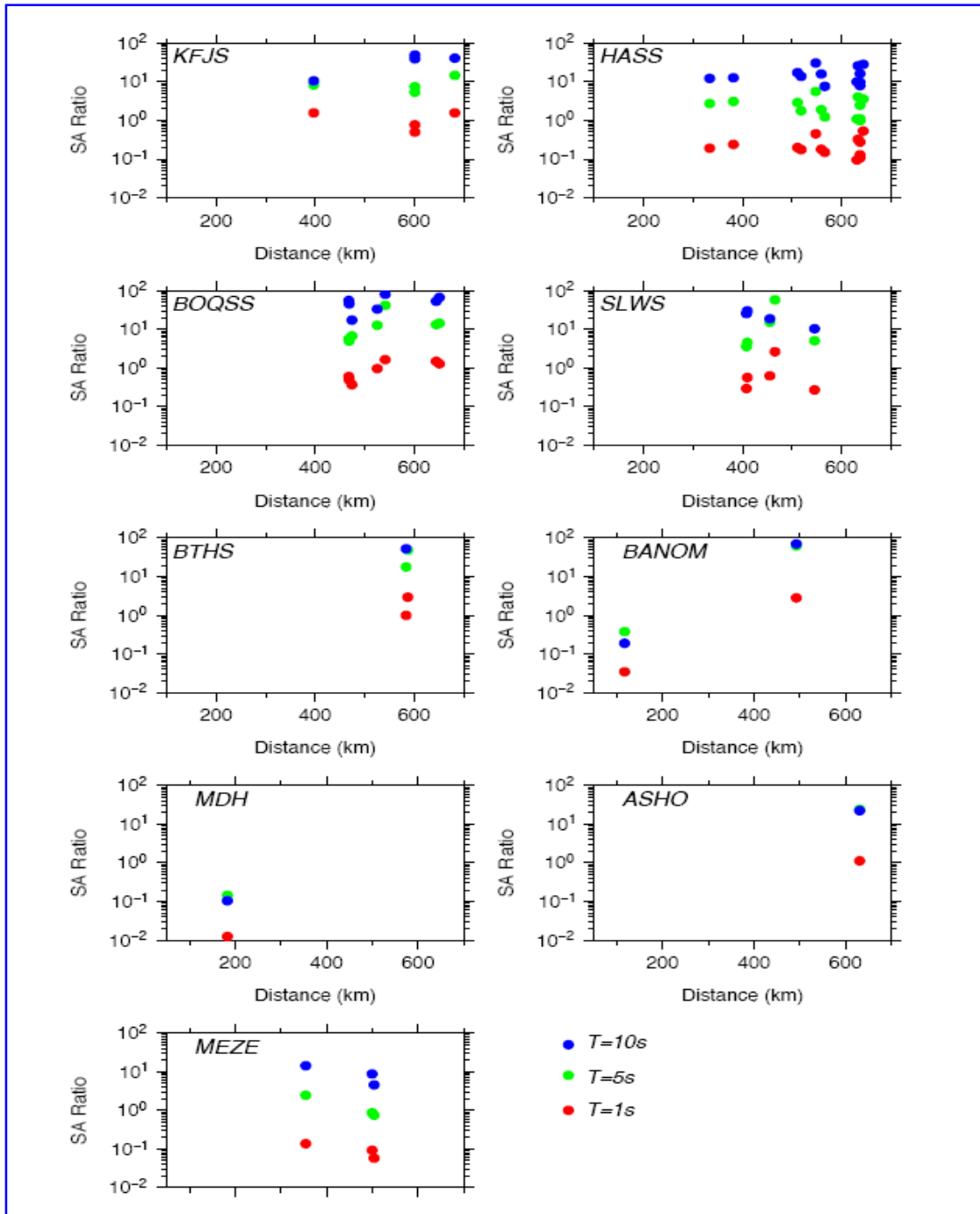


Figure 6.5 Spectral acceleration ratios of recorded and predicted ground motion for the geometric mean horizontal component at periods 1s, 5s, and 10s, and 5% damping. The predicted ground motion was computed using the GMP of Campell and Bozorgnia (2008). The stations name is indicated in each panel.

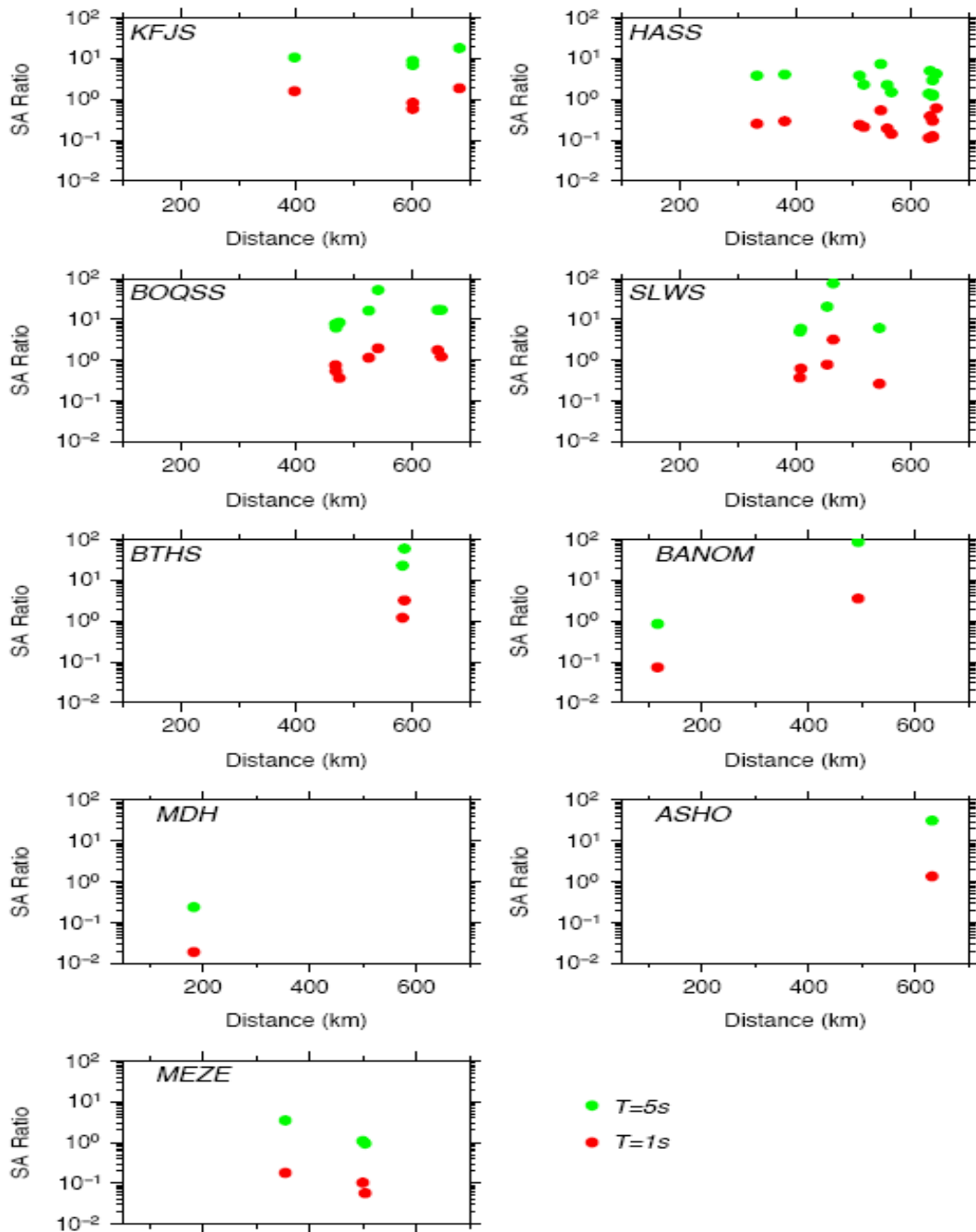


Figure 6.6. Mean spectral acceleration ratios of recorded and predicted ground motion at periods of 1s, 5s, and 5% damping. The predicted ground motion was computed using the GMP of Atkinson and Boore developed for Eastern North America (2006). The stations name is indicated in each panel.

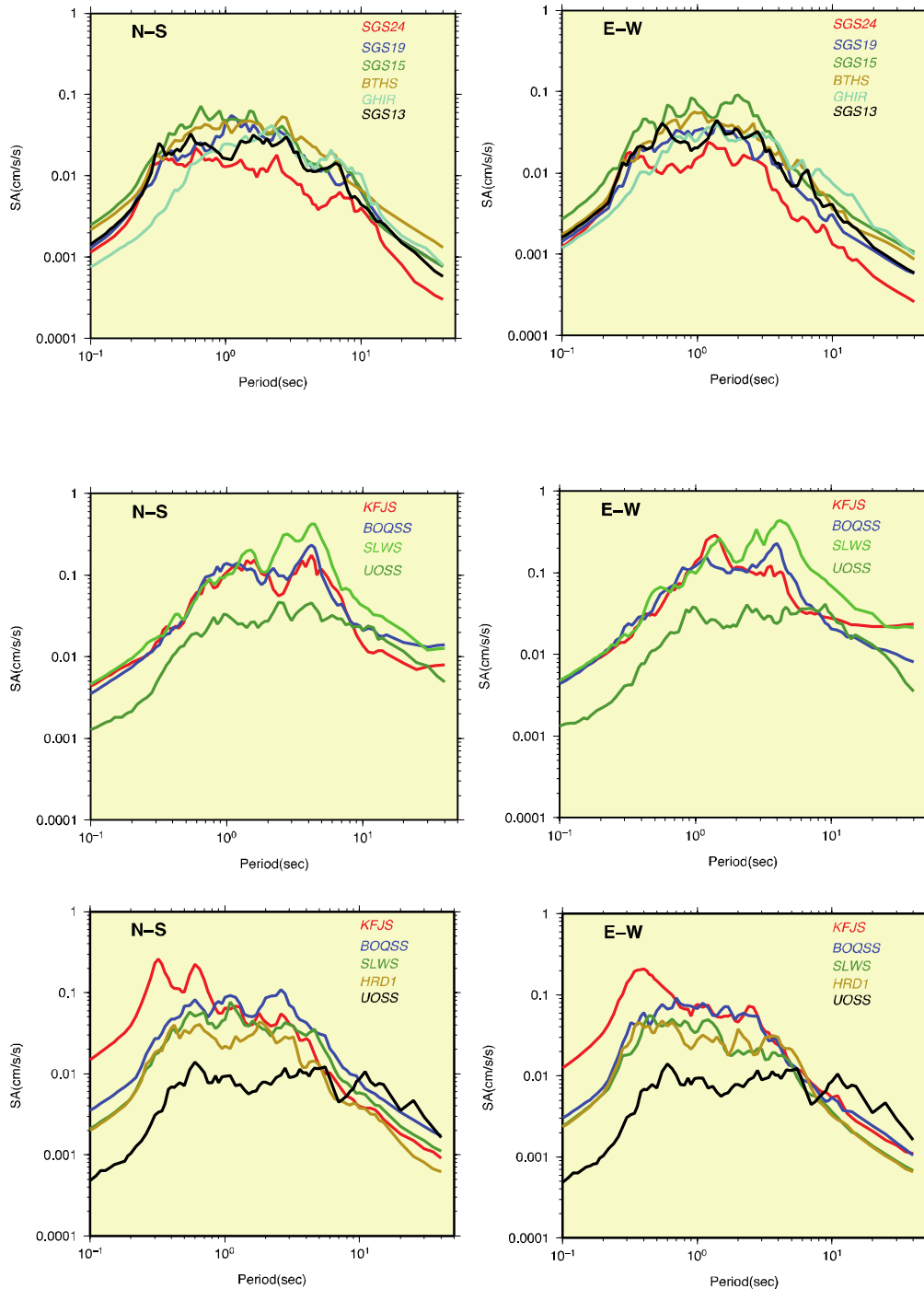


Figure 6.7 Acceleration response spectra for ground motion from M 5.3 2006/06/03 earthquake (top panels), M5.7 2010/07/20 (middle panels), M 5.9 2010/09/27 (bottom panels), recorded at different stations in the Gulf region. The names of the stations are shown in each panel.

6. 4 Modeling of Long-Period Ground Motions in the Gulf

We modeled long-period ground motions with the available models of 3D crustal velocity and attenuation structure. We used also source parameters from events determine earlier in the project. We performed simulations of observed seismograms on high-performance computers at LLNL and ported codes to high-performance computers at KSU and installed the 3D-FDM WPP computer program used in the simulations.

In order to understand the nature of the long-duration and increased amplitude of ground motion in the Gulf basin, we simulated wave propagation in three-dimensional earth models using a finite-difference technique. In the future we plan to use validated velocity models such as LITHO1.0 to compute strong ground motion for large scenario earthquakes in the region.

We modeled elastic seismic wave propagation by using WPP, a computer code developed at Lawrence Livermore National Laboratory (Petersson and Sjogreen, 2010a). WPP is an anelastic finite difference code based on a second- order accurate scheme (Nilsson et al., 2007) including mesh refinement (Petersson and Sjogreen;2010b)and a boundary conforming grid for the topographic free surface boundary condition (Appelo and Petersson , 2008). The code is designed specifically for use on massively parallel machines and has the capability to handle complex topography. WPP has been tested and validated against other numerical techniques, and has been used to model ground motion from large earthquakes in California, such as the 1906 San Francisco earthquake (Aagaard et al., 2008).

The preliminary 3D seismic velocity models used here are based on 2D cross sections of the sedimentary basin thickness reported by Laske and Masters(1997). **Figure 6.8** shows cross sections of three basin velocity models. In Model 1 the surface sedimentary layer continues

across the entire model. In Model 2 the surface sedimentary layer has limited extension toward the west. In Model 3 the geometry of the eastern basin edge is modified so that it can better channel the seismic energy coming from the seismic source below. All three geometries represent possible characteristics of the basin structure in the Gulf region, which are not well resolved in current basin models. The multiple realizations of the basin geometry and different spatial extensions of surface sedimentary layers in 3D ground motion simulations can improve our understanding of the influence of the sedimentary basin structure on seismic waves propagation in the Arabian Peninsula. Our goal is to replicate both the frequency response and the duration of the observed seismograms using our modeling techniques.

6.5 3-D Ground Motion Simulation

3-D ground motion simulations at periods of practical interest and for large regions require massive parallel computing. In this study the maximal modeled frequency is 0.4 Hz. We used a grid spacing of 200m in the top 10 km of the model, and 400m in the region below 10km. All simulations with WPP code were performed on 500 computer nodes.

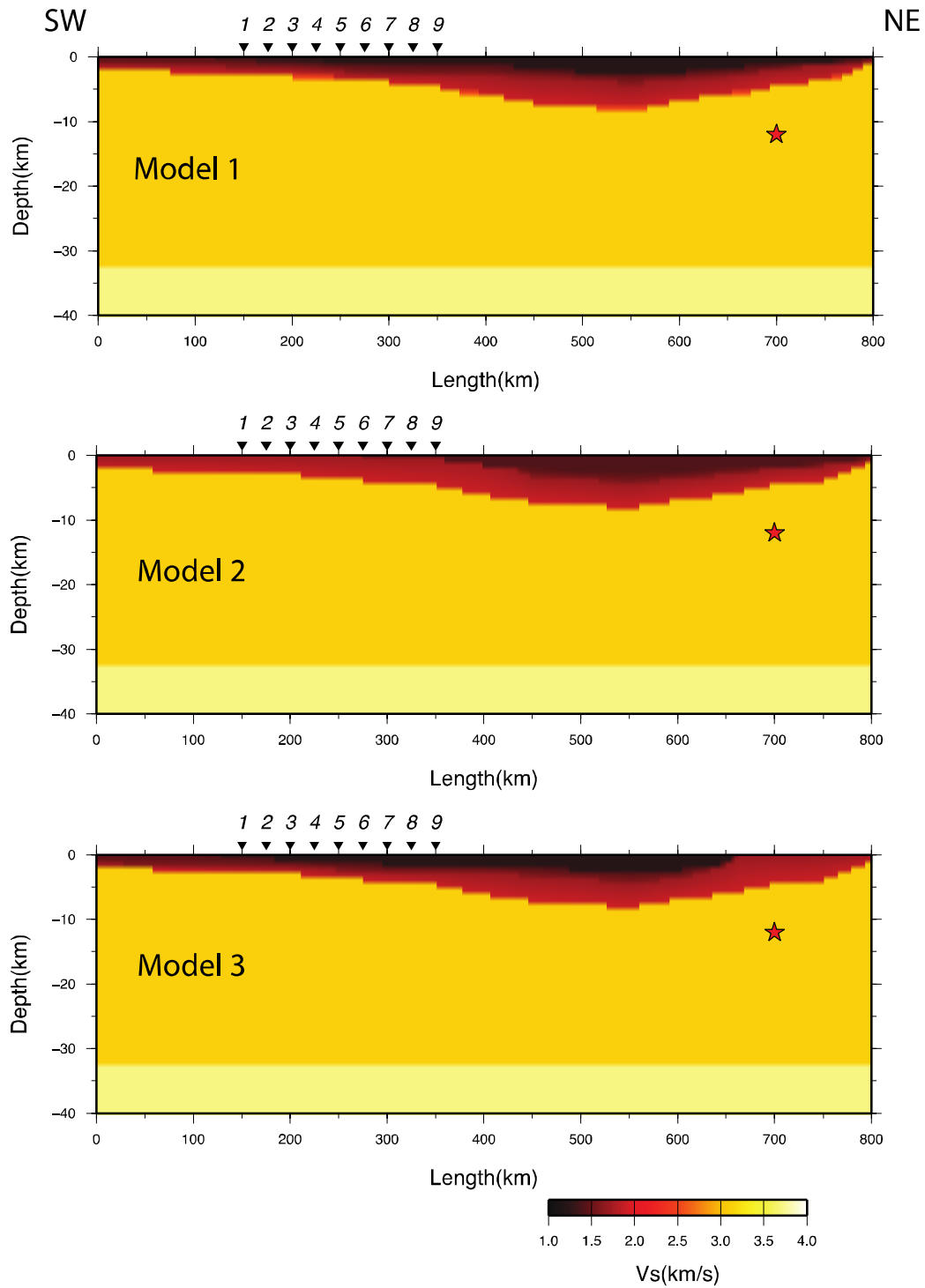


Figure 6.8. Vertical cross sections of three velocity models used in the simulation of basin generated waves. Star indicates the location of the double couple point source.

Figure 6.9 shows synthetic velocity seismograms computed for a Mw5.4 double couple point source with a thrust mechanism using Model 1, Model 2, and Model 3. The top sedimentary layer in our velocity models has a $V_p=2.2$ km/s, $V_s=1.2$ km/s, density 2 g/cm³, $Q_p=200$ and $Q_s=100$. The source depth is 12 km. We used a Gaussian source time function with predominant frequency of 1Hz. Note that only stations 1 and 2 have epicentral distances over 500 km. Their epicentral distance is in the range of distances of stations located on the west side of the Gulf from earthquakes in the Zagros region. The simulations reproduce the duration of the ground motion observed at such distances. The duration of the simulated ground motion increases with distance, and the basin-trapped waves are clustered in different wave trains that relate with different basin layers in our model. Here we focus on long period waves. We band-pass filtered the synthetic seismograms in two frequency ranges 0.1-0.4 Hz (2.5s-10s period range) and 0.02-0.05 Hz (20s-50s period range). The comparisons between the three models in two frequency ranges are shown in **Figures 6.10a and 6.10b**. The long period surface waves (20-40 s) are only affected by the deep basin structure. They are very similar for all models. The effect of structural complexities in the shallow basin sedimentary layers is observed at relatively short periods, especially in the vertical component of motion (**Figure 6.11**). The differences among the basin models become significant at station 1 and 2 which record waves that travels across the entire basin structure. These simulations illustrate the significant effect of shallow sedimentary layers on ground motion duration and amplitude in the period range of 2.5s-10s.

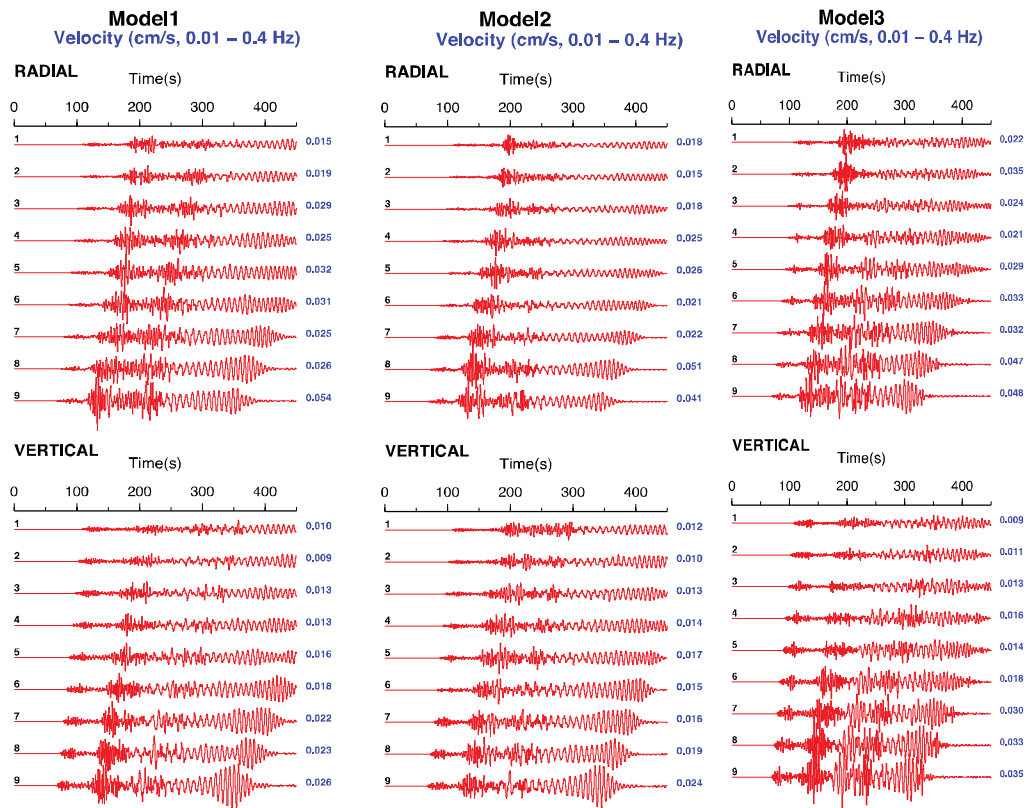


Figure 6.9 Synthetic velocity seismograms computed for a double couple point source with a thrust mechanism using Model 1 (left panels) Model 2 (central panels), and Model 3 (right panels). The seismograms are band-pass filtered at 0.01-0.4 Hz.

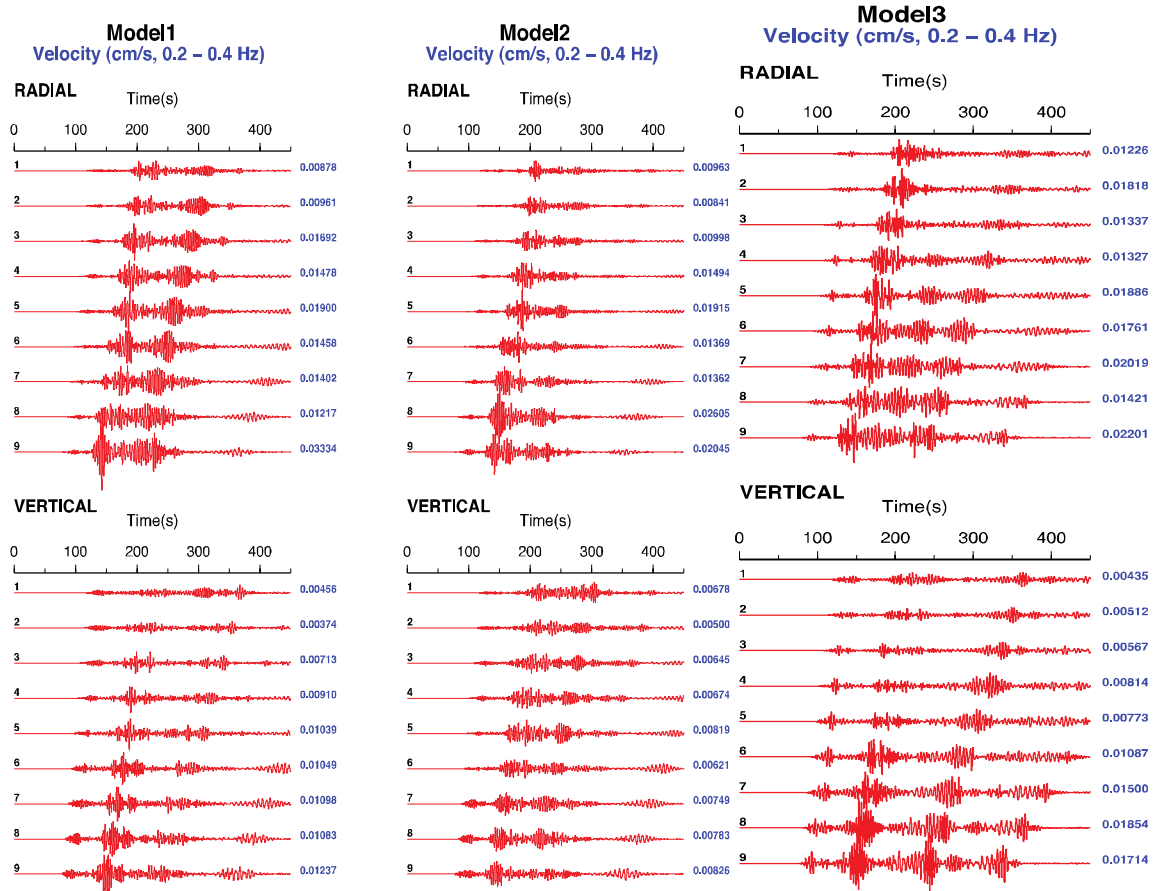


Figure 6.10a. Synthetic velocity seismograms computed for a double couple point source with a thrust mechanism using Model 1 (left panels) and Model 2 (central panels), and Model 3 (right panels). The seismograms are band-pass filtered at 0.2-0.4 Hz.

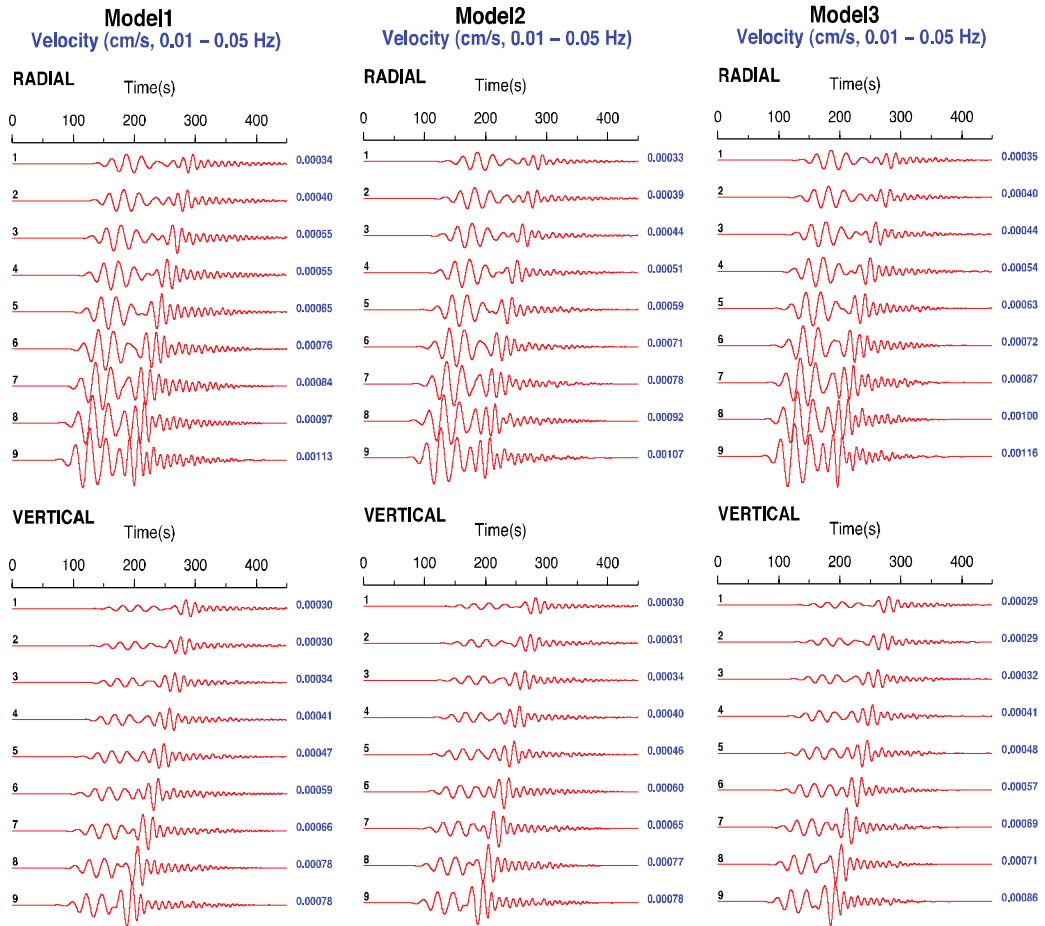


Figure 6.10b. Same as 6.10a, but band-pass filtered at 0.01-0.05 Hz.

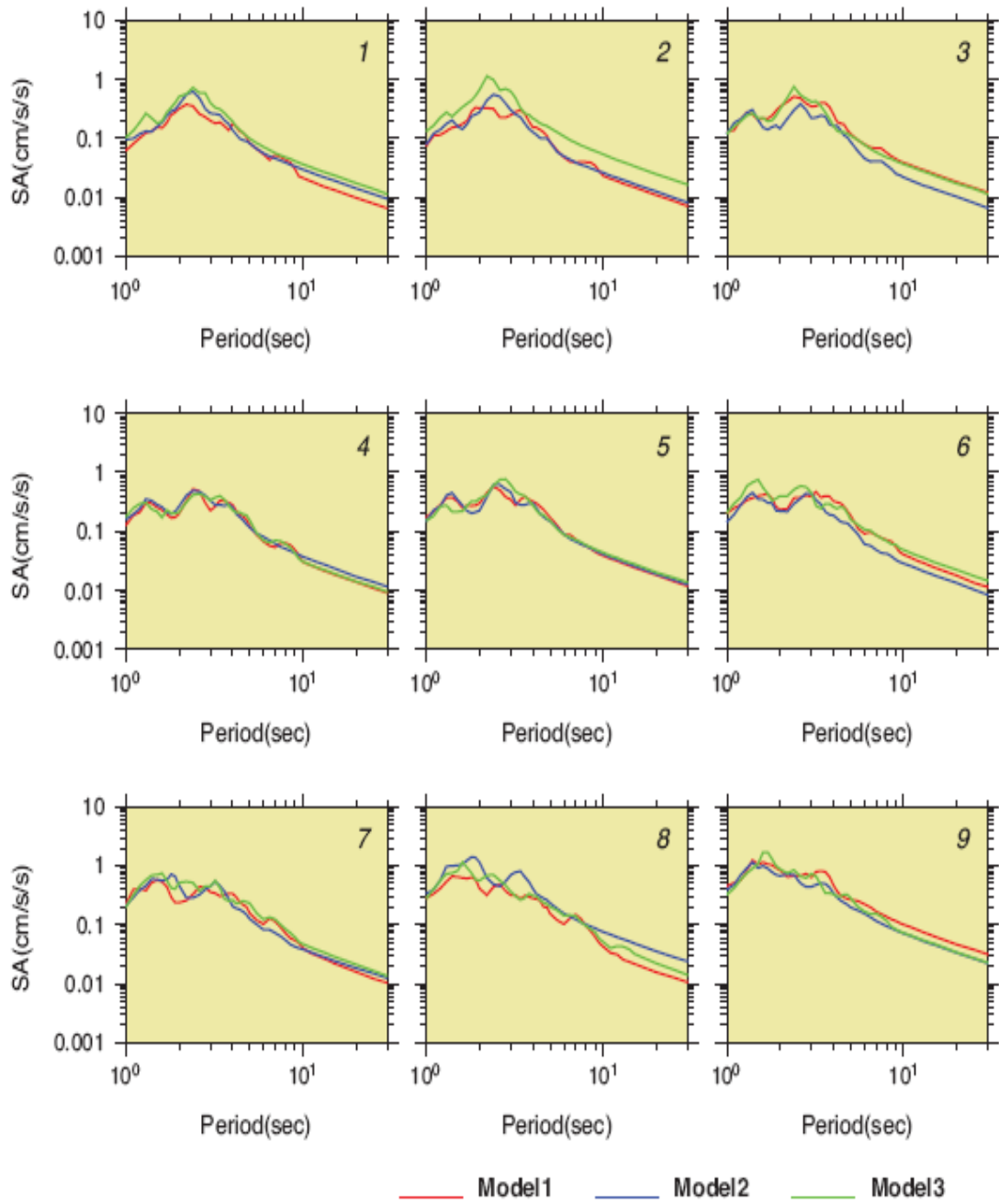


Figure 6.11. Comparison acceleration response spectra of synthetic seismograms shown in Figure 6.9 for Model 1 (red traces), Model 2 (blue traces), and Model 3 (green traces).

6.6 Ground Motion Simulation Using LITHO1.0

Simulations were run through a preliminary version of the velocity model LITHO1.0 (Pasyanos et al., 2012). The LITHO1.0 is an update of the crustal models CRUST5.1 (Mooney et al., 1998) and CRUST2.0 (Bassin et al., 2000), but at higher (1°) resolution and extended deeper into the mantle to include the lithospheric lid and asthenosphere layers. Unlike the previous models, it is driven by its ability to fit a recently developed high-resolution surface wave dispersion model (Ma et al., 2012) which includes both Love and Rayleigh, and both group and phase velocity, over a wide frequency band (5 mHz – 40 mHz). Sedimentary structure, which is important for the simulations presented here, are derived from the 1° sediment model of Laske and Masters (1997). Although the shear wave velocity of the basin sedimentary layers in the original LITHO1.0 model is as low as 525 m/s near the free surface, in our simulations we limit the shear wave velocity to 1200m/s. Using a minimum grid spacing of 200m the corresponding maximal modeled frequency is 0.4 Hz. A vertical cross-section of the model is shown in **Figure 6.12**. The increase of shear wave velocity in the top sedimentary layers decreases both the amplitude and duration of basin secondary waves. This is mainly caused by the weakening of the wave trapping mechanism caused by the reduction of the velocity contrast between shallow and deeper sedimentary layers.

Figure 6.13 shows the synthetic ground motion computed with LITHO1.0. LITHO1.0 produces ground motion waveforms that are similar to ones simulated with Model1. The most significant differences between the two models are seen at short periods 1-3s for which LITHO1.0 produces much larger ground motion (see response spectra in **Figure 6.14**). LITHO1.0 produces ground motion that is consistent with the observed ones. For example the shape of response spectra at

station 1 and 3 which correspond to station SGS 13 and BTHS for the M5.3, 2006/06/03 earthquake, compare well with spectra of E-W component (see **Figure 6.7**).

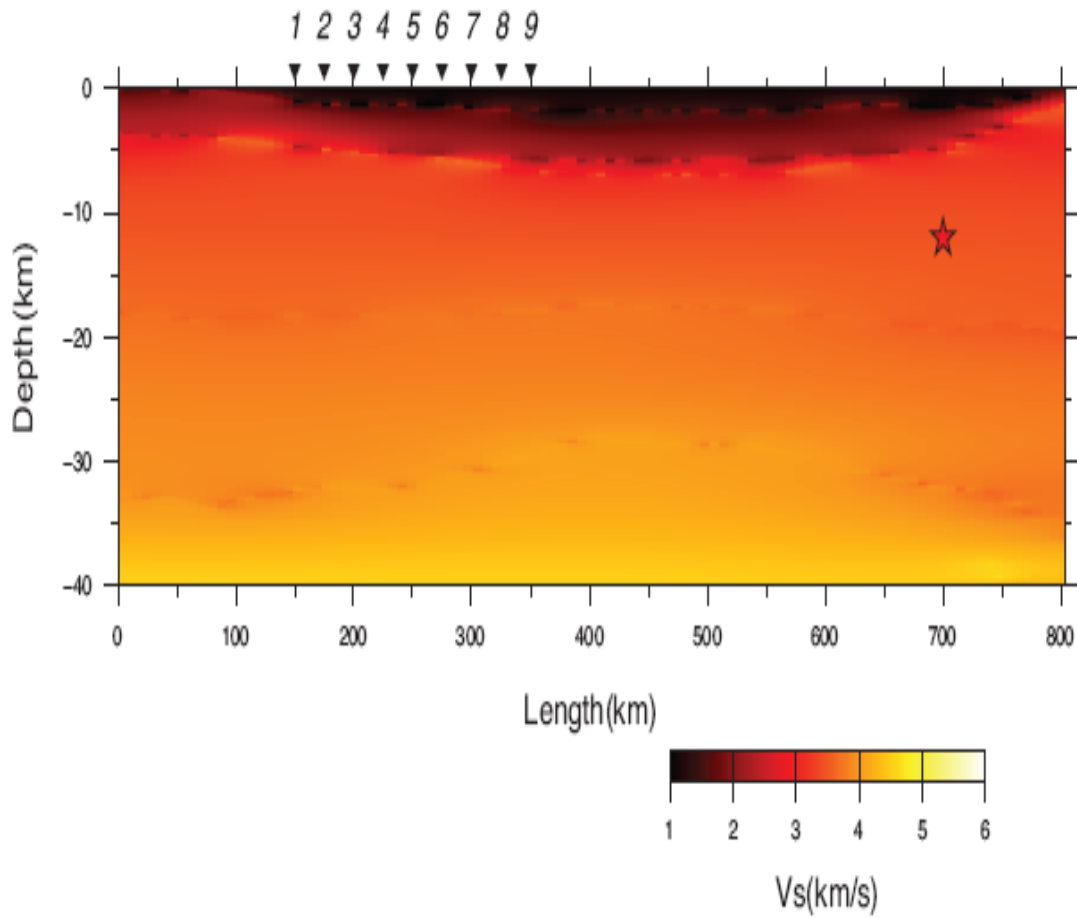


Figure 6.12. Vertical cross section of the tomographic model used in the simulation of basin-generated waves.

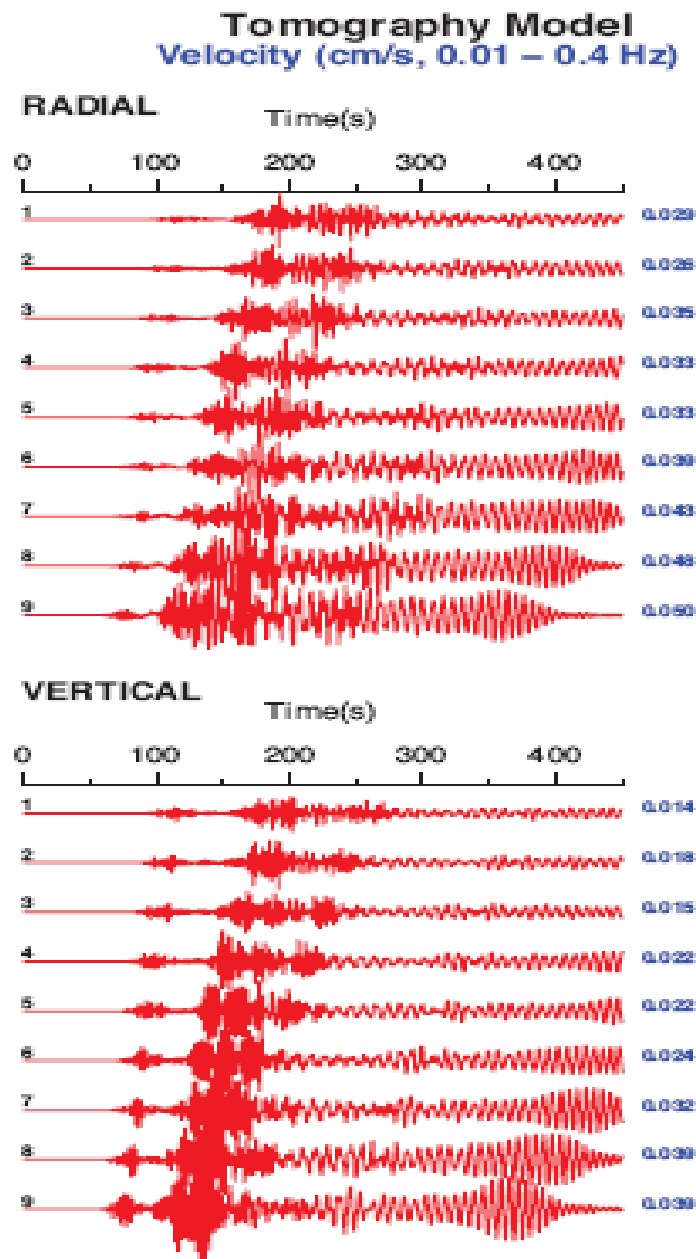


Figure 6.13. Synthetic velocity seismograms computed for a double couple point source with a trust mechanism using tomographic model.

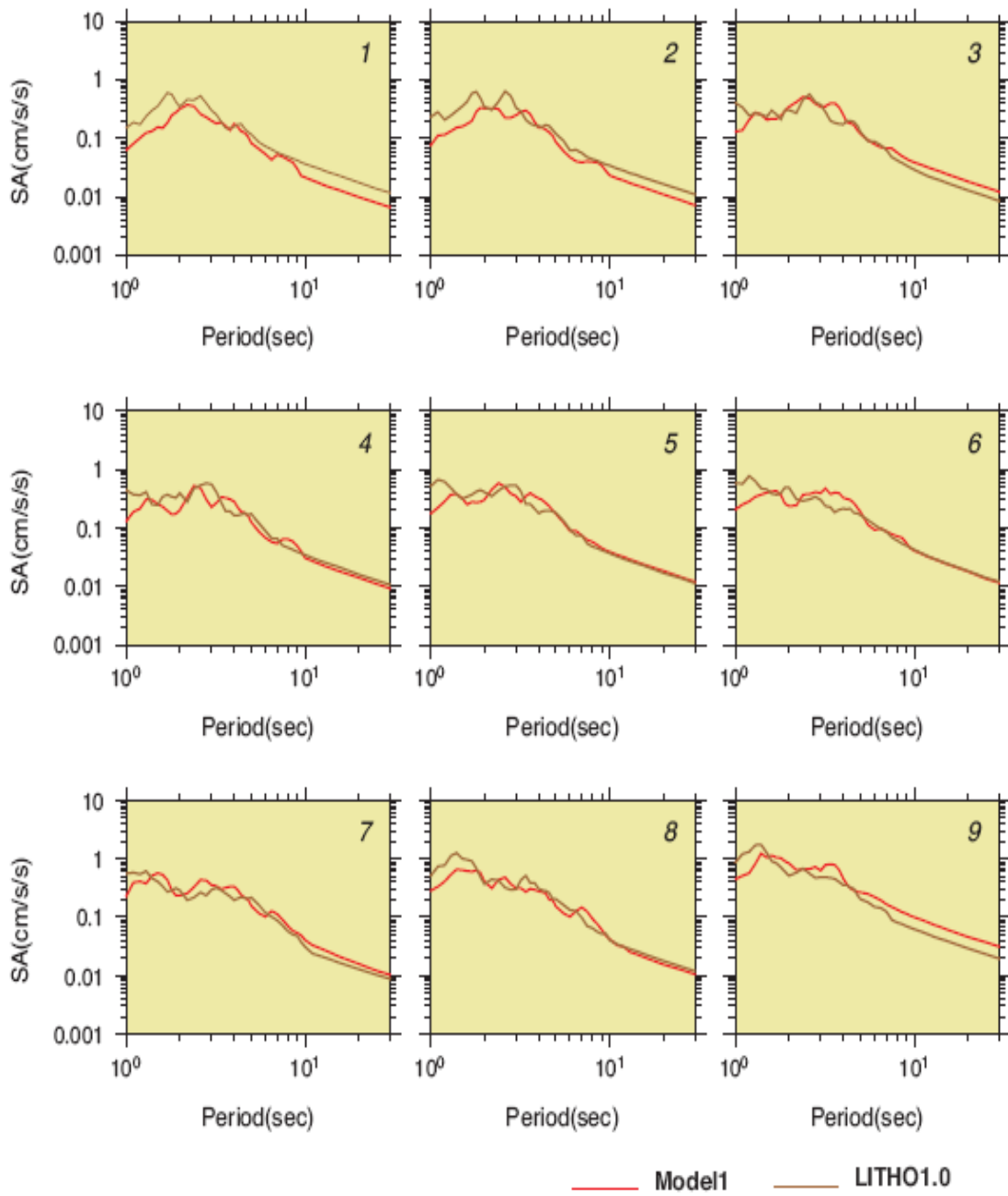


Figure 6.14 Comparison of acceleration response spectra of synthetic seismograms computed with the tomographic model and three other basin models.

Summary & Conclusions

We have obtained new waveform data from stations in the Arabian Peninsula and have made thousands of surface wave dispersion measurements. These measurements are used to create updated Rayleigh and Love wave group velocity maps which have high-resolution over a wide period band. Surface wave amplitude measurements which are used in tomography for surface wave attenuation are more difficult to make than group velocity dispersion measurements because information about the source amplitude is needed, requiring a moment tensor solution. Having a focal mechanism is also needed to avoid making measurements at radiation nodes, where amplitudes can be contaminated by multi-pathing. Moment tensor solutions have been determined using regional waveform methods, complementing the large number of Global CMT solutions in the region. Surface wave attenuation maps based on the path measurements from stations in Saudi Arabia and nearby countries were presented, compared and contrasted with our dispersion maps and analyzed for information about the attenuation properties of the sediments, crystalline crust, and upper mantle of the Arabian Peninsula.

Comparisons with two commonly used GMPEs performed in Task 3 showed that ground motion recorded in the Gulf region from earthquakes in the Zagros region is highly anomalous. The recorded peak ground motion is much higher than the predicted one in the period range 1-10s. The extraordinary duration of the seismic energy in this frequency band may have a significant impact on large structures along the Gulf shoreline. We speculate that both duration and amplitude of the ground motion is due to waveguide effects in the sedimentary structure of the Gulf basin.

This hypothesis was tested in Task 4 using large-scale 3D waveform modeling and different basin models, including the recently developed model LITHO1.0. Sensitivity analysis of the

basin induced waves and the corresponding response spectra due to complexities in the shallow basin structure reveal the significance of 3D basin models in predicting strong ground motion in the Gulf region. Our simulations suggest that a plausible explanation of the anomalous observed ground motion is the generation of basin reverberation waves that are trapped in the shallow sedimentary layers of the basin. We also found that in order to explain the very large duration of ground motion the quality factors Q_p and Q_s in the top sedimentary layers should be at least 200 and 100, respectively.

Since we focused on ground motion at very large distances, our simulations were performed using point source representation. Future simulations of well-recorded earthquakes in the Gulf region should use LITHO1.0 model and kinematic rupture models of earthquake sources. A better representation of the shallow crustal structure and source process will improve the quality of the ground motion simulation on a broad period range.

Generally speaking :

- Long-period ground motions are of concern in the Gulf region
 - Basin structure traps and amplifies surface waves
 - Tall structures are particularly vulnerable to 2-10 second periods
- Numerical simulation of seismic wave propagation
 - Is important to understand seismic response
 - Provides predictive capability for likely scenario earthquakes
 - Extension of Seismic Hazard Assessment (SHA) should account for deterministic, scenario earthquake ground motions
- Large earthquakes in the Makran (or Zagros) could have wide spread, far-reaching damage
- Improved models of seismic velocity structure will improve accuracy of numerical simulations
 - We need more accurate basin depth and velocity models
 - Oil & Gas industry data

- Geotechnical (shallow) shear velocities
- Models must be validated with ground motion observations

Future work : In order to fully understanding the detail seismological and seismic hazard picture of the Arabian Gulf region, this study recommends an extensive research covering installation of strong motion accelerographs along the coastal areas of the Gulf which is of great importance to precisely estimate the attenuation characteristics of the region and to improve seismic hazard and building code parameters.

REFERENCES

- Aagaard, B., et al. (2008), Ground motion modeling of the 1906 SanFrancisco earthquake II: Ground motion estimates for the 1906 earthquake and scenario events, *Bull. Seismol. Soc. Am.*, 98, 10121046,doi:10.1785/0120060410.
- Alamri, A. (2013). Seismotectonics and seismogenic source zones of the Arabian Platform, K. Al Hosani et al. (eds.), *Lithosphere Dynamics and Sedimentary Basins: The Arabian Plate and Analogues*, *Frontiers in Earth Sciences*, DOI: 10.1007/978-3-642-30609-9_15, _ Springer-Verlag Berlin Heidelberg.
- Al-Amri, A.M. (1998). The crustal structure of the western Arabian Platform from the spectral analysis of long-period P-wave amplitude ratios, *Tectonophysics*, **290**, 271-283.
- Al-Amri, A.M. (1999). The crustal and upper-mantle structure of the interior Arabian platform, *Geophysical Journal International*, **136**,421-430.
- Al-Amri, A. L., R. Mellors, and F. L. Vernon (1999). Broadband Seismic Noise Characteristics of the Arabian Shield, *Arabian Journal of Science and Engineering*, King Fahd University of Petroleum and Minerals, 24, 99-113.
- Al-Amri,A., Rodgers A., and Al-Khalifah, T.(2008). Improving the level of seismic hazard parameters in Saudi Arabia using earthquake location, *Arabian Journal of Geosciences*, Volume 1, Number 1, doi: 10.1007/s12517-008-0001-5
- Al-Amri, A., Harris D., Fnais M., Rodgers A., and Hemida M (2012). A regional seismic array of three-component stations in central Saudi Arabia. *Seismological Research Letters*, V. 83, No. 1, 49 – 58.
- Al-Damegh, K., E. Sandvol, and M. Barazangi (2005). Crustal structure of the Arabian Plate: new constraints from the analysis of teleseismic receiver functions, *Earth Planet. Sci. Letts.*, 231, 177-196.
- Al-Damegh, K., Sandvol, E., Al-Lazki, A. and Barazangi, M. (2004). Regional wave propagation (Sn and Lg) and Pn attenuation in the Arabian plate and surrounding regions, *Geophys. J. Int.*, **157**, 775-795.
- Al-Damegh, K. S.; AbouElenean, K. M.; Hussein, H. M.; Rodgers, A. J. (2008). Source mechanisms of the June 2004 Tabuk earthquake sequence, Eastern Red Sea margin, Kingdom of Saudi Arabia, *Journal of Seismology*, Volume 13, Issue 4, pp.561-576
- Al-Husseini M I (2000) Origin of the Arabian plate structures: Amar collision and Najd rift, *GeoArabia*, 5(4), 527-542
- Appelo, D., and N. A. Petersson (2008), A stable finite difference methodfor the elastic wave equation on complex geometries with free surfaces, *Commun. Comput. Phys.*, 5, 84–107.

Badri, M. (1991). Crustal structure of central Saudi Arabia determined from seismic refraction profiling, *Tectonophysics*, 185, 357-374.

Bassin, C. G. Laske, and G. Masters (2000). The current limits of resolution in surface wave tomography in North America, *EOS Trans. AGU*, F897, 81.

Benoit, M., A. Nyblade, J. VanDecar, H. Gurrola (2003). Upper mantle P wave velocity structure and transition zone thickness beneath the Arabian Shield, *Geophys. Res. Lett.* 30, 1-4.

Boore and Atkinson (2006), Earthquake Ground-Motion Prediction Equations for Eastern North America. *Bull. Seism. Soc. Am.*, 96, no6, 2181-2205.

Campbell and Bozorgnia (2008) NGA ground motion model for the geometric mean horizontal component of PGA, PGV, PGD and 5% damped linear elastic response spectra for periods ranging from 0.01 to 10 s. *Earthquake Spectra*, 24, No1, 139-171.

Debayle, E., J. Leveque, M. Cara, Seismic evidence for a deeply rooted low-velocity anomaly in the upper mantle beneath the northeastern Afro/Arabian continent (2001). *Earth Planet. Sci. Lett.* 193, 423-436.

Dreger, D., Helmberger, D., 1993. Determination of source parameters at regional distances with single station or sparse network data. *J. Geophys. Res.* 98, 8107 – 8125.

Gettings, M., H. Blank, W. Mooney and J. Healey (1986). Crustal structure of southwestern Saudi Arabia, *J. Geophys. Res.*, 91, 6491- 6512.

Komatitsch, D. and Tromp, J., 2002a. Spectral-element simulations of global seismic wave propagation-i.validation, *Geophys. J. Int.*, 149, 390–412.

Komatitsch, D. and Tromp, J., 2002b. Spectral-element simulations of global seismic wave propagation-ii.three-dimensional models, oceans, rotation and self-gravitation, *Geophys. J. Int.*, 150, 303–318.

Laske, G. and T.G. Masters (1997). A global digital map of sediment thickness, *EOS Trans. AGU*, 78, F483, <http://igppweb.ucsd.edu/~gabi/sediment.html>

Looseveld R J H, Bell A, Terken J J M (1996) The tectonic evolution of interior Oman, *GeoArabia*, 1 (1), 28-51

Ma, Z. et al (2012). In preparation

Mellors, R., Vernon, F., Camp, V., Al-Amri, A.M and Gharib, A. (1999). Regional waveform propagation in the Saudi Arabian Peninsula and evidence for a hot upper mantle under western Arabia. *J. Geophys. Res.*, 104, 20,221–20,235

- Moktar, T. A., C. J. Ammon, R. B. Herrmann and H. A. A. Ghalib (2001) Surface wave velocities across Arabia. *Pure. Appl. Geophys.*, 158, 1425-1444.
- Mooney, W.D., G. Laske, and G. Masters (1998). CRUST5.1: A global crustal model at 5°×5°, *J. Geophys. Res.*, 103, 727-747.
- Mooney, M. Gettings, H. Blank, J. Healy, Saudi Arabian seismic refraction profile: A traveltime interpretation of crustal and upper mantle structure (1985). *Tectonophysics* 111, 173-246.
- Nilsson, S., N. A. Petersson, B. Sjogreen, and H.-O. Kreiss (2007), Stable difference approximations for the elastic wave equation in second order formulation, *SIAM J. Numer. Anal.*, 45, 1902–1936, doi:10.1137/060663520.
- Park, Y., A. Nyblade, A. Rodgers and A. M Al-Amri (2007). Upper mantle structure beneath the Arabian Peninsula from regional body-wave tomography: Implications for the origin of Cenozoic uplift and volcanism in the Arabian Shield, *Geochemistry, Geophysics, Geosystems*, 8, doi:10.1029/2006GC001566.
- Pasyanos, M.E., E.M. Matzel, W.R. Walter, and A.J. Rodgers (2009a). Broadband Lg attenuation modeling of the Middle East, *Geophys. J. Int.*, 177, 1166-1176, doi: 10.1111/j.1365-246X.2009.04128.x
- Pasyanos, M.E., W.R. Walter, and E.M. Matzel (2009b). A simultaneous multi-phase approach to determine P-wave and S-wave attenuation of the crust and upper mantle, *Bull. Seism. Soc. Amer.*, 99-6, DOI: 10.1785/0120090061.
- Pasyanos, M.E., T.G. Masters, G. Laske, and Z. Ma (2012). LITHO1.0: An updated crust and lithospheric model of the Earth, in preparation.
- Peterson., J. (1993). Observations and modeling of seismic background noise, USGS Open-File Report 93-322.
- Petersson, N. A., and B. Sjogreen (2010a), Reference guide to WPP version 2.0, Tech Rep. LLNL-TR-422928, Lawrence Livermore Natl. Lab., Livermore, Calif.
- Petersson N.A., and B. Sjogreen (2010b). Stable grid refinement and singular source discretization for seismic wave simulations. *Communications in Computational Physics*, vol. 8, no. 5, pp. 1074-1110.
- Pitarka, A., K. Irikura, T. Iwata and H. Sekiguchi (1998). Three-dimensional simulation of the near-fault ground motion for the 1995 Hyogo-ken Nanbu (Kobe), Japan, earthquake. *Bull. Seism. Soc. Am.*, **88**, 428-440.
- Powers R W, Ramirez L F, Redmond C D, Elberg E L (1966). Geology of the Arabian Peninsula, Sedimentary geology of Saudi Arabia: USGS professional paper 560-D D1-D147

- Ritsema, J., Lay, T., 1995. Long-period regional wave moment tensor inversion for earthquakes in the western United States. *J. Geophys. Res.* 100, 9853 – 9864.
- Rodgers, A., W. Walter, R. Mellors, A. M. S. Al-Amri and Y. S. Zhang (1999). Lithospheric structure of the Arabian Shield and Platform from complete regional waveform modeling and surface wave group velocities, *Geophys. J. Int.*, 138, 871-878.
- Rodgers, A. J., N. A. Petersson, and B. Sjogreen (2010). Simulation of topographic effects on seismic waves from shallow explosions near the North Korean nuclear test site with emphasis on shear wave generation. *Bull. Seism. Soc. Am.*, 115, B11309.
- Rodgers, A.J., A. Fowler, A.S. Al-Amri, and A. Al-Enezi (2006). The March 11, 2002 Masafi, United Arab Emirates earthquake: Insights into the seismotectonics of the northern Oman Mountains. *Tectonophysics*, 415 (2006) 57–64.
- Rodgers, A.J., J.F. Ni, and T. M. Hearn (1997). Propagation characteristics of short-period Sn and Lg in the Middle East, *Bull. Seism. Soc. Am.* 87, 396-413
- Sandvol, E., D. Seber, M. Barazangi, F. Vernon, R. Mellors and A. Al-Amri (1998). Lithospheric discontinuities beneath the Arabian Shield, *Geophys. Res. Lett.*, 25, 2873-2877.
- Talebian, M., and J. Jackson (2004), A reappraisal of earthquake focal mechanisms and active shortening in the Zagros mountains of Iran, *Geophys. J. Int.*, 156, 506 – 526.
- Tkalčić H., M. Pasyanos, A. Rodgers, R. Gok and A. Al-Amri (2006). A multi-step approach for joint modeling of surface wave dispersion and teleseismic receiver functions: Implications for lithospheric structure of the Arabian Peninsula. *J. Geophys. Res.*, 111, B113111, doi:10.1029/2005JB004130.
- Vernon, F., and J. Berger (1997). Broadband seismic characterization of the Arabian Shield, Final Scientific Technical Report, Department of Energy Contract No. F 19628-95-K-0015, 36 pp.
- Walter, W.R. and S.R. Taylor (2001). A revised magnitude and distance amplitude correction (MDAC2) procedure for regional seismic discriminants: theory and testing at NTS, Lawrence Livermore National Laboratory, UCRL-ID-146882
<http://www.llnl.gov/tid/lof/documents/pdf/240563.pdf>
- Zhao, L.-S. and D. Helmberger (1994). Source estimation from broadband regional seismograms, *Bull. Seis. Soc. Am.*, 84, 91-104.
- Zhu, L., and D. V. Helmberger (1996). Advancements in source estimation techniques using broadband regional seismograms, *Bull. Seis. Soc. Am.*, 86, 1634-1641.

PUBLICATIONS / PRESENTATIONS

1. PUBLICATIONS

As we stated in the original proposal, we plan to publish at least two papers from the outcome of the project in peer-review journals of high impact factor.

2. PRESENTATIONS

We presented the outcome of the project and acknowledged NPST in the following conferences.

- A. American Geophysical Union, San Francisco, CA, Dec. 12-16 , 2011
- B. 4th International Professional Geology, Vancouver, Canada, January 22 -24, 2012.
- C. Gulf Seismic Forum, Muscat, Oman, March 3 - 6, 2013.
- D. American Geophysical Union, Cancun, Mexico, May 19 - 23, 2013